

- Takeya, H., Onose, R., Osada, H., 1998. Caspase-mediated activation of a 36-kDa myelin basic protein kinase during anticancer drug-induced apoptosis. *Cancer Res.* 58, 4888–4894.
- Karin, M., Greten, F.R., 2005. NF- κ B: linking inflammation and immunity to cancer development and progression. *Nat. Rev. Immunol.* 5, 749–759.
- Kataoka, T., 2005. The caspase-8 modulator c-FLIP. *Crit. Rev. Immunol.* 25, 31–58.
- Kataoka, T., 2009. Chemical biology of inflammatory cytokine signaling. *J. Antibiot.* 62, 655–667.
- Lamberti, A., Caraglia, M., Longo, O., Marra, M., Abbruzzese, A., Arcari, P., 2004. The translation elongation factor 1A in tumorigenesis, signal transduction and apoptosis: review article. *Amino Acids* 26, 443–448.
- Lindqvist, L., Robert, F., Merrick, W., Takeya, H., Fraser, C., Osada, H., Pelletier, J., 2010. Inhibition of translation by cytotrienin A—a member of the ansamycin family. *RNA* 16, 2404–2413.
- Liu, C., Xu, P., Lamouille, S., Xu, J., Derynck, R., 2009. TACE-mediated ectodomain shedding of the type I TGF- β receptor downregulates TGF- β signaling. *Mol. Cell* 35, 26–36.
- Mateyak, M.K., Kinzy, T.G., 2010. eEF1A: thinking outside the ribosome. *J. Biol. Chem.* 285, 21209–21213.
- Ogura, H., Tsukumo, Y., Sugimoto, H., Igarashi, M., Nagai, K., Kataoka, T., 2008a. Ectodomain shedding of TNF receptor 1 induced by protein synthesis inhibitors regulates TNF- α -mediated activation of NF- κ B and caspase-8. *Exp. Cell Res.* 314, 1406–1414.
- Ogura, H., Tsukumo, Y., Sugimoto, H., Igarashi, M., Nagai, K., Kataoka, T., 2008b. ERK and p38 MAP kinase are involved in downregulation of cell surface TNF receptor 1 induced by acetylcycloheximide. *Int. Immunopharmacol.* 8, 922–926.
- Roebuck, K.A., Finnegan, A., 1999. Regulation of intercellular adhesion molecule-1 (CD54) gene expression. *J. Leukoc. Biol.* 66, 876–888.
- Seals, D.F., Courtneidge, S.A., 2003. The ADAMs family of metalloproteases: multi-domain proteins with multiple functions. *Genes Dev.* 17, 7–30.
- Shifrin, V.I., Anderson, P., 1999. Trichothecene mycotoxins trigger a ribotoxic stress response that activates c-Jun N-terminal kinase and p38 mitogen-activated protein kinase and induces apoptosis. *J. Biol. Chem.* 274, 13985–13992.
- Sidhu, J.S., Omiecinski, C.J., 1998. Protein synthesis inhibitors exhibit a nonspecific effect on phenobarbital-inducible cytochrome P450 gene expression in primary rat hepatocytes. *J. Biol. Chem.* 273, 4769–4775.
- Soond, S.M., Everson, B., Riches, D.W.H., Murphy, G., 2005. ERK-mediated phosphorylation of Thr735 in TNF- α -converting enzyme and its potential role in TACE protein trafficking. *J. Cell Sci.* 118, 2371–2380.
- Sugimoto, H., Kataoka, T., Igarashi, M., Hamada, M., Takeuchi, T., Nagai, K., 2000. E-73, an acetyl analogue of cycloheximide, blocks the tumor necrosis factor-induced NF- κ B signaling pathway. *Biochem. Biophys. Res. Commun.* 277, 330–333.
- Takada, Y., Matsuo, K., Ogura, H., Bai, L., Toki, A., Wang, L., Ando, M., Kataoka, T., 2009. Odoroside A and ouabain inhibit Na⁺/K⁺-ATPase and prevent NF- κ B-inducible protein expression by blocking Na⁺-dependent amino acid transport. *Biochem. Pharmacol.* 78, 1157–1166.
- Watabe, M., Takeya, H., Onose, R., Osada, H., 2000. Activation of MST/Krs and c-Jun N-terminal kinases by different signaling pathways during cytotrienin A-induced apoptosis. *J. Biol. Chem.* 275, 8766–8771.
- Xu, P., Derynck, R., 2010. Direct activation of TACE-mediated ectodomain shedding by p38 MAP kinase regulates EGF receptor-dependent cell proliferation. *Mol. Cell* 37, 551–566.
- Yamada, Y., Tashiro, E., Taketani, S., Imoto, M., Kataoka, T., 2011. Mycotrienin II, a translation inhibitor that prevents ICAM-1 expression by pro-inflammatory cytokines. *J. Antibiot* 64, 361–366.
- Yamamoto, K., Tashiro, E., Imoto, M., 2011. Quinotriexin inhibits ER-stress-induced XBP1 mRNA splicing through inhibition of protein synthesis. *Biosci. Biotechnol. Biochem.* 75, 284–288.
- Zhang, H.P., Takeya, H., Osada, H., 1997. Novel triene-ansamycins, cytotrienins A and B, inducing apoptosis on human leukemia HL-60 cells. *Tetrahedron Lett.* 38, 1789–1792.

Roles of Porphyrin and Iron Metabolisms in the δ -Aminolevulinic Acid (ALA)-induced Accumulation of Protoporphyrin and Photodamage of Tumor Cells

Yoshiko Ohgari¹, Yoshinobu Miyata¹, Taeko Miyagi¹, Saki Gotoh¹, Takano Ohta¹, Takao Kataoka¹, Kazumichi Furuyama² and Shigeru Taketani^{*1,3}

¹Department of Biotechnology, Kyoto Institute of Technology, Kyoto, Japan

²Department of Molecular Biology and Applied Physiology, Tohoku University Graduate School of Medicine, Sendai, Miyagi, Japan

³Insect Biomedical Center, Kyoto Institute of Technology, Kyoto, Japan

Received 13 April 2011, accepted 29 May 2011, DOI: 10.1111/j.1751-1097.2011.00950.x

ABSTRACT

δ -Aminolevulinic acid (ALA)-induced porphyrin accumulation is widely used in the treatment of cancer, as photodynamic therapy. To clarify the mechanisms of the tumor-preferential accumulation of protoporphyrin, we examined the effect of the expression of heme-biosynthetic and -degradative enzymes on the ALA-induced accumulation of protoporphyrin as well as photodamage. The transient expression of heme-biosynthetic enzymes in HeLa cells caused variations of the ALA-induced accumulation of protoporphyrin. When ALA-treated cells were exposed to white light, the extent of photodamage of the cells was dependent on the accumulation of protoporphyrin. The decrease of the accumulation of protoporphyrin was observed in the cells treated with inducers of heme oxygenase (HO)-1. The ALA-dependent accumulation of protoporphyrin was decreased in HeLa cells by transfection with HO-1 and HO-2 cDNA. Conversely, knock-down of HO-1/-2 with siRNAs enhanced the ALA-induced protoporphyrin accumulation and photodamage. The ALA effect was decreased with HeLa cells expressing mitoferrin-2, a mitochondrial iron transporter, whereas it was enhanced by the mitoferrin-2 siRNA transfection. These results indicated that not only the production of porphyrin intermediates but also the reuse of iron from heme and mitochondrial iron utilization control the ALA-induced accumulation of protoporphyrin in cancerous cells.

INTRODUCTION

Photodynamic therapy (PDT) was developed as treatment of nonmelanoma skin tumors and preneoplastic skin lesions. PDT includes the activation of photosensitizer, which causes the release of singlet oxygen and other reactive oxygen species upon exposure to light, resulting in photodamage of cells, followed by tissue destruction (1). In tumor cells, *via* the heme biosynthesis pathway, photosensitizer protoporphyrin is synthesized from a large amount of exogenous ALA and accumulates in a specific manner (2). The application of ALA following PDT treatment has been used in the treatment of

skin diseases and has advantages over systemic administration in that the entire body does not face sensitization (3,4). ALA-induced PDT has been successfully applied in various medical fields, including urology, gastroenterology and dermatology (3–5). In heme biosynthesis, ALA is catalyzed by four cytosolic enzymes, ALA-dehydratase, porphobilinogen deaminase (PBGD), uroporphyrinogen synthase (UROS) and uroporphyrinogen decarboxylase and by two mitochondrial enzymes, coproporphyrinogen oxidase (CPOX) and protoporphyrinogen oxidase (PPOX), converting to protoporphyrin (6). Finally, ferrochelatase (FECH) catalyzes the insertion of ferrous ions into protoporphyrin to produce heme (7). Although there are reports that ALA-induced PDT can also be used as a fluorescence detection marker for the photodiagnosis of tumors (3,4,8), the mechanisms involved in the specific accumulation of protoporphyrin in cancerous tissues have not been clearly demonstrated. Previously, we (7,8) reported that protoporphyrin accumulates owing to limited capacity for the FECH reaction. In addition, we also reported an increase in the uptake of ALA by cancerous cells (8).

Heme oxygenase (HO) is the rate-limiting enzyme in the cellular catabolism of heme to biliverdin, carbon monoxide and free iron. Biliverdin is subsequently converted to bilirubin by biliverdin reductase (9,10). The enzyme is expressed in a variety of organisms. In mammals, two HO isoforms, HO-1 and HO-2, have been reported. The expression of HO-1 is induced by heme, a substrate of the enzyme and metal ions, such as arsenite and cadmium, whereas that of HO-2 is constant (10). Interestingly, most of the known HO-1 inducers stimulate the production of ROS or lead to a depletion of glutathione levels, indicating the involvement of the induction of HO-1 in cellular protection against oxidative stress (11,12). The induced HO-1 could have an advantage in cell growth, resulting in a protective effect against the photosensitivity of tumors, whereas the knockdown of HO-1 gives rise to suppression of cell growth with failure in the photosensitivity (13). In contrast, the reduced expression of HO-1 mRNA by siRNA increased cell death upon ALA-PDT (14). Thus, the effect of the expression of HO-1 on ALA-PDT is inconclusive. Furthermore, the contribution of HO-2 to the effectiveness of ALA-PDT is unclear.

*Corresponding author email: taketani@kit.ac.jp (Shigeru Taketani)

© 2011 The Authors

Photochemistry and Photobiology © 2011 The American Society of Photobiology 0031-8655/11

Iron utilization in mitochondria in cancerous cells also remains poorly understood. It was shown that functions of the respiratory chain enzymes including iron- or heme-containing proteins were impaired in tumors (15). As for mitochondrial iron metabolism, mitoferrin, a mitochondrial iron importer, transports iron in mitochondria and can regulate iron-chelation into protoporphyrin by FECH (16). Mitoferrin-1 is synthesized in erythroid cells, whereas mitoferrin-2 is synthesized in various tissues (16). Otherwise, iron delivery to the iron-sulfur cluster biosynthetic machinery can be mediated by frataxin, a mitochondrial iron-chaperon (17). The reduction of the expression of frataxin causes Friedreich's ataxia, an inherited neurodegenerative disorder (17). Targeted disruption of frataxin in murine hepatocytes causes decreased life span and increased liver tumor formation, whereas the over expression of frataxin leads to inhibition of cell growth of cancer, by increasing oxidative phosphorylation (18). Thus, iron deficiency related to FECH in cancerous cells may be responsible for the ALA-induced accumulation of protoporphyrin. Previous studies (8,19) also showed that removal of iron from the cells with an iron chelator, desferrioxamine, markedly enhanced the ALA-induced accumulation of protoporphyrin. However, as desferrioxamine has a protective effect against phototoxicity *in vitro* and *in vivo*, it did not appear to confer additional benefit in ALA-PDT (20). Therefore, it is necessary to clarify the utilization of mitochondrial iron for heme production. In this study, we investigated the role of the utilization of iron and the recycling of iron from heme for the ALA-induced accumulation of protoporphyrin and photodamage. Down-regulation of the expression of iron-metabolizing molecules mitoferrin-2, frataxin and HO-1/-2 increased the ALA-induced photodamage, whereas up-regulated expression gave the reverse effect. The importance of increased expression of porphyrin-metabolizing enzymes on ALA-PDT was also shown.

MATERIALS AND METHODS

Materials. Protoporphyrin IX, cobalt-protoporphyrin (Co-PP) and tin-protoporphyrin (Sn-PP) were purchased from Frontier Scientific Co. (Logan, UT). The antibodies for HO-1, HO-2 and actin used were as previously described (10). Monoclonal antibodies for frataxin and HA were products of Millipore Co. (Billerica, MA) and MBL Laboratories (Tokyo, Japan), respectively. HO-1 (No. sc-44306), frataxin (No. sc-40580), mitoferrin-2 (No. sc-90800) and control siRNAs (No. sc-37007) were products of Santa Cruz Biotechnology (Santa Cruz, CA). HO-2 siRNA was synthesized by Sigma-Aldrich (Tokyo, Japan): sense r(CCACCACGGGCACUUUACUUA) and antisense r(AAGUAAAGUGCCGUGGCGC). All other chemicals used were of analytical grade.

Plasmids. Plasmids pcDNA3-HF (human FECH) (8), pcDNA3-HCPOX (human CPOX) (21), pCD-PPOX (human PPOX) (22), pCAG-HMBSu (human nonerythroid PBGD) (23) and pCAG-UROS (human nonerythroid UROS) (23) were used for the expression of enzymes in cells. Plasmids pHHO-1 and pHHO-2 carrying human HO-1 and HO-2 cDNAs, respectively, were kind gifts from Dr. Shibahara (24,25). To construct pcDNA3-frataxin, PCR was performed with mouse liver cDNA library. Primers 5'-AAGGATCCATGTGGACTCTCGGGCGC-3' and 5'-AAGGATCCTCAAGCATCTTTCCGG A-3' were used. Amplified cDNAs were digested with *Bam*HI and ligated into *Bam*HI-digested pcDNA3. To obtain the full-length cDNA fragment of human mitoferrin-2, PCR reaction was performed with the following primers: 5'-AATCTAGAGAGTTGGAGGG GCGGGGT-3 and 5'-AAAAGCTTGCCAGCCCTCCACTCT-3' for mitoferrin-2 and human kidney cDNA library as a template. Then, to make mammalian expression vector carrying mitoferrin-2 containing

an HA-tag at the C-terminus, the amplified cDNA was ligated into the *Xba*I/*Hind*III site of the vector pCG-C-HA (26).

Cell cultures. Human epithelial cervical cancer HeLa cells were grown in Dulbecco's modified Eagle's medium (DMEM) supplemented with fetal calf serum (FCS) and antibiotics. The cells (1×10^5) in a 1.5-cm-diameter dish were transfected using Lipofectamine 2000 (Invitrogen Co., San Jose, CA) with the indicated plasmid then incubated in the presence of 10% FCS at 37°C for 16–24 h (26). The cells also transfected with siRNAs were cultured for 48 h. The cells were then incubated in the absence or presence of ALA (0.5–1 mM) for 16 h before being exposed to light, as described previously (7,8).

Exposure of the cells to light. The cells were incubated with ALA (1 mM) for 8–16 h and 1.0 mL of fresh drug-free medium was then added. Irradiation with visible light was carried out under sterile conditions, using a fluorescence lamp, in a CO₂ incubator, as described previously (8,27). Cell viability was measured by 3-(4,5-dimethylthiazol-2-yl)-2,5-diphenyl-2H-tetrazolium bromide (MTT) assay. Each experiment was carried out in triplicate or quadruplicate. Cell viability (cell survival) is expressed as a percentage of control cells. Porphyrins were extracted from the cells with 96% ethanol containing 0.5 M HCl (8). The amount of protoporphyrin was determined by fluorescence spectrophotometry, as previously described (8,27).

Immunoblotting. The lysates from HeLa cells were subjected to sodium dodecylsulfate-polyacrylamide gel electrophoresis (SDS-PAGE) and electroblotted onto poly(vinylidene difluoride) (PVDF) membrane (Bio-Rad Laboratories, Hercules, CA). Immunoblotting was carried out with antibodies for HO-1, HO-2, HA, frataxin and actin, as the primary antibodies (8).

Reverse transcriptase (RT)-PCR analysis. Total RNA was isolated from the cells by the guanidium isothiocyanate method (26). Single-strand cDNA derived from the RNA was synthesized with the oligo (dT) primer, using ReveTra Ace (Toyobo, Co., Tokyo, Japan), followed by PCR, using the indicated primers. The amount of cDNA added to the reaction mixture was normalized by the intensity of glyceraldehyde-3-phosphate dehydrogenase (GAPDH) amplicon. The cDNAs obtained were analyzed using a 1% agarose gel and electrophoresed. The primers were 5'-CCGGGGCCGGGGACCTTAG-3' (forward) and 5'-GCGGGTACCCACGCGAATCAC-3' for PBGD, 5'-CCCCATCGGAAATTGCTTAGG-3' (forward) and 5'-CTTTCC CAGACTTCAGTTTATTG-3' for UROS, 5'-ATGTTGCCTAAGA GACCTC-3' (forward) and 5'-ACAAAATGGCAATTTACC-3' for CPOX, 5'-CCCACAGCCAGACTCAGC-3' (forward) and 5'-GCTG TTAGGTTCTGTGCC-3' for PPOX, 5'-GTGCAAAACCTCAAG TT-3' (forward) and 5'-TCACAGCTCTGGCTGGT-3' for FECH, 5'-ATGTGGACTCTCGGGCGC-3' (forward) and 5'-CTCAAGCA TCTTTTCCGGA-3' for frataxin, 5'-GAGTTGGAGGGGCGGG GT-3' (forward) and 5'-GCCAGCCCTCCACTCT-3' for mitoferrin-2 and 5'-TGGGTGTGAACCACGAGA-3' (forward) and 5'-TTACT CCTTGAGGCCATG-3' for GAPDH.

RESULTS

Effect of the expression of porphyrin-biosynthetic enzymes on the ALA-induced accumulation of protoporphyrin and photodamage in HeLa cells

Previously, we (8) reported that the decrease of the expression of FECH led to enhancement of the ALA-induced accumulation and photodamage. To examine whether other heme-biosynthetic enzymes are involved in the enhancement of ALA-induced accumulation of protoporphyrin, HeLa cells were transfected with pcDNA3-HF, pcDNA3-HCPOX, pCD-PPOX, pCAG-HMBSu and pCAG-UROS. The expression of these enzymes was not examined owing to lack of availability of the corresponding antibody, but RT-PCR analysis showed the increased expression of the corresponding transcript by transfection (Fig. 1A). The cells were incubated with 1 mM ALA and the accumulation of protoporphyrin was examined.

As shown in Fig. 1B, the highest accumulation of protoporphyrin in PBGD-transiently expressing cells was observed

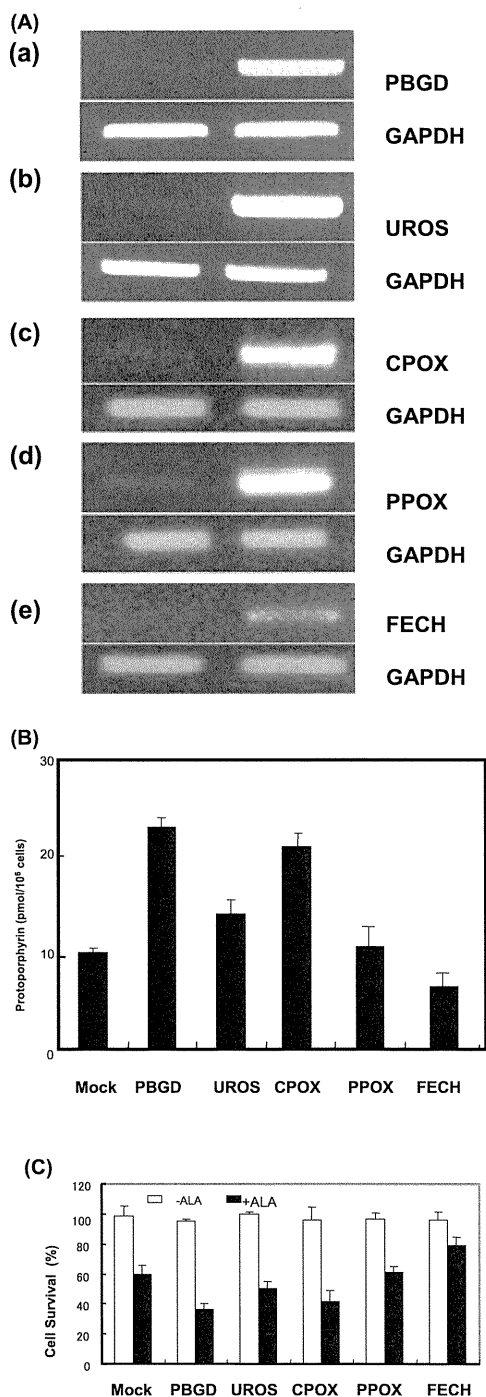


Figure 1. Effect of the expression of heme-biosynthetic enzymes on ALA-induced accumulation of protoporphyrin and photodamage in HeLa cells. (A) HeLa cells were transfected with pcDNA3-HF, pcDNA3-HCPOX, pCD-PPOX, pCAG-HMBSu and pCAG-UROS. After 16-h incubation, RNA was isolated and treated with DNase I. RT-PCR for PBGD (a), UROS (b), CPOX (c), PPOX (d) and FECH mRNA (e) was performed; (B) Effect of the expression of PBGD, UROS, CPOX, PPOX and FECH on the ALA-induced accumulation of protoporphyrin. HeLa cells (5×10^5) transfected with the indicated plasmids were incubated for 24 h and treated with 1 mM ALA for 16 h. The cells were washed twice with phosphate-buffered saline, then porphyrin was extracted and measured fluorospectrophotometrically; (C) Photosensitivity. Fresh DMEM was added to the cells treated as above, followed by exposure to white light; then surviving cells were assessed by MTT assay. Data are the mean \pm SD of three independent experiments.

compared with that in control cells. The expression of UROS or CPOX also increased the accumulation. The accumulation in FECH-expressing cells was decreased, whereas that in PPOX-expressing cells was similar to that in the control. When enzyme-expressing cells were exposed to white light and photodamage was examined, the extent of cell survival was found to be related to low accumulation of protoporphyrin (Fig. 1C). No significant cell death was observed by irradiation minus ALA or by treatment with ALA minus light (data not shown). These results indicated that increase in the expression of heme-biosynthetic enzymes, including PBGD, UROS and CPOX led to high accumulation of protoporphyrin.

Involvement of iron reutilization from heme in ALA-induced accumulation of protoporphyrin and photodamage in HeLa cells

To examine if iron-containing compounds decrease the accumulation of protoporphyrin from ALA, HeLa cells were incubated with 0.5 mM ALA by the addition of 10 μ M hemin or 50 μ M Fe-NTA for 16 h. Porphyrins were extracted from the cells and determined. As shown in Fig. 2A, the

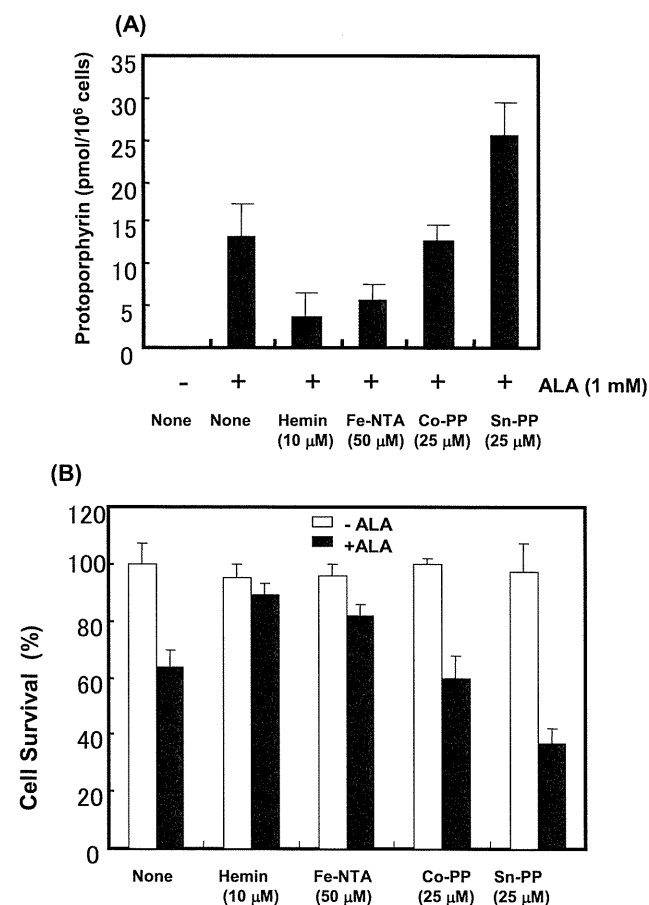


Figure 2. Effect of metalloporphyrins and Fe-NTA on ALA-induced accumulation of protoporphyrin and photodamage. (A) Effect of hemin, Fe-NTA, Co-PP and Sn-PP on the ALA-induced accumulation of protoporphyrin. HeLa cells (5×10^5) were incubated with 1 mM ALA plus the indicated concentration of chemicals for 16 h. Porphyrin was extracted from the cells and measured using a fluorospectrophotometer; (B) Effect of hemin, Fe-NTA, Co-PP and Sn-PP on ALA-induced photodamage. The cells treated as above were irradiated, and survival of the cells was analyzed by MTT assay. Data are the mean \pm SD of three to four independent experiments.

accumulation of ALA-induced protoporphyrin in hemin- or ferric ion-nitrilotriacetate (Fe-NTA)-treated cells was decreased, compared with that in ALA-treated cells. Sn-PP, an inhibitor of HO, increased the accumulation of protoporphyrin. Co-PP, a substrate of HO, was without effect on the accumulation. When the ALA-induced photodamage was examined, hemin and Fe-NTA reduced the photodamage dependent on the decrease of protoporphyrin (Fig. 2B). Sn-PP but not Co-PP increased the photodamage. The above results suggest that the generation of iron from heme may decrease the photodamage and accumulation of protoporphyrin.

Our previous studies (28,29) showed that treatment of the cells with hemin and metal ions resulted in the induction of HO-1. When the cells were treated with hemin, arsenite or cadmium ions for 16 h, HO-1 was markedly induced (Fig. 3A). The ALA-induced accumulation of protoporphyrin in arsenite and cadmium ion-treated cells was decreased compared with that in the control, but the extent was less than that in the case of hemin (Fig. 3A). These results suggest that reutilization of iron generated from heme by HO led to the decrease of the accumulation of protoporphyrin. Then, the HeLa cells were transfected with pHHO-1 or pHHO-2. As shown in Fig. 3B, the expression of HO-1 and HO-2 by the transfection was increased. When the cells were then treated with ALA, the accumulation of protoporphyrin in HO-1 or HO-2-expressing cells was decreased, indicating that the increase in the expression of HOs can facilitate the recycling of iron from heme. These observations led us to examine if knockdown of the HO-1/-2 expression affects the accumulation of protoporphyrin. When HeLa cells were transfected with HO-1/-2 siRNAs and incubated for 48 h, the levels of HO-1 and HO-2 proteins were markedly decreased (Fig. 4A). After the

subsequent 16-h incubation with ALA, the content of porphyrin was measured. As expected, the accumulation of protoporphyrin was increased by knockdown of HO-1 and HO-2 (Fig. 4B). The photodamage by HO-1/-2 double knockdown was much greater than that by transfection of control RNA (Fig. 4C). These results indicate that cessation of the recycling of iron from heme enhances the ALA-induced photodamage.

Involvement of mitochondrial iron-metabolizing proteins in regulating the ALA-induced accumulation of protoporphyrin and photodamage

Recently, some researchers (16) reported that mitochondrial iron-metabolizing proteins including mitoferrin-2 and frataxin regulate heme and Fe-S cluster biosynthesis. To clarify the involvement of these proteins in the ALA-induced accumulation of protoporphyrin, HeLa cells transiently expressing frataxin or nonerythroid type mitoferrin-2 were made (Fig. 5A). After these cells were incubated with ALA for 16 h, porphyrin in the cells was examined. The expression of mitoferrin-2, but not frataxin, decreased the ALA-induced accumulation of protoporphyrin in a dose-dependent manner (Fig. 5B). The ALA-induced photodamage with these cells was also examined. The light-resistant cells were increased dependent on the decrease of protoporphyrin (Fig. 5C). Finally, knockdown of the expression of frataxin and mitoferrin-2 using siRNA was carried out (Fig. 6A). The ALA-induced accumulation of protoporphyrin in frataxin- or mitoferrin-2-deficient cells was more than that of control cells (Fig. 6B). Upon exposure of the cells to light, photodamage of frataxin- or mitoferrin-2-deficient cells was greater than that of the

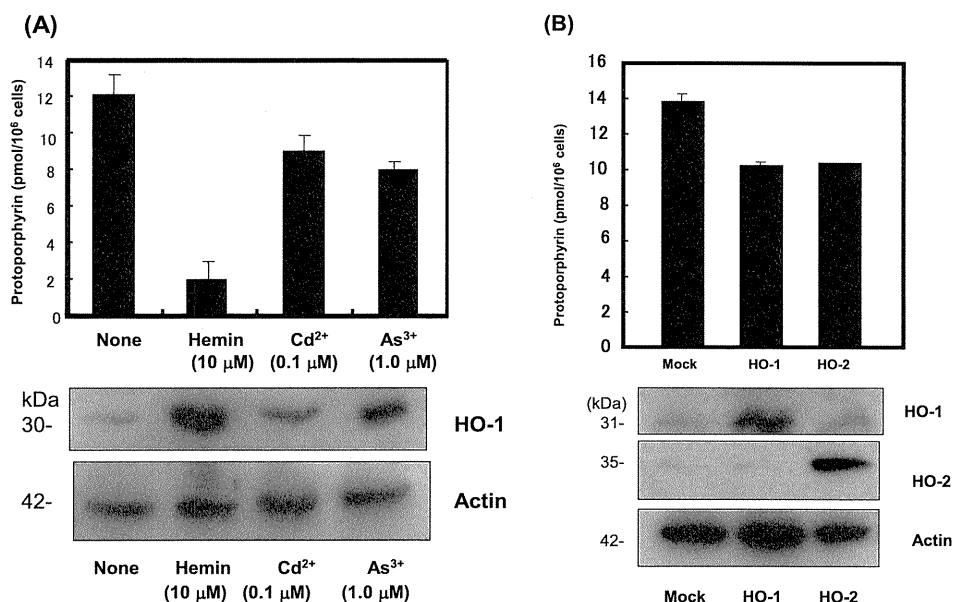


Figure 3. Reduction of ALA-induced accumulation of protoporphyrin and photodamage by the expression of HO-1,-2. (A) Effect of hemin, sodium arsenite and cadmium chloride on the ALA-dependent accumulation of protoporphyrin. Upper panel: HeLa cells (5×10^5) were treated with the above chemicals at the indicated concentration plus 1 mM ALA for 16 h. The accumulated protoporphyrin was measured. Data are the mean \pm SD of three independent experiments. Lower panels: Immunoblots of HO-1. Cell lysates from cells treated with hemin, sodium arsenite and cadmium chloride for 16 h were analyzed by SDS-PAGE, followed by immunoblotting; (B) Effect of over expression of HO-1 and HO-2 on the accumulation of protoporphyrin. The cells transfected with pHHO-1 and pHHO-2 were cultured for 16 h, followed by incubation with 1 mM ALA for 8 h. Upper panel: Porphyrin was extracted and determined. Lower panel: Immunoblots of HO-1 and HO-2.

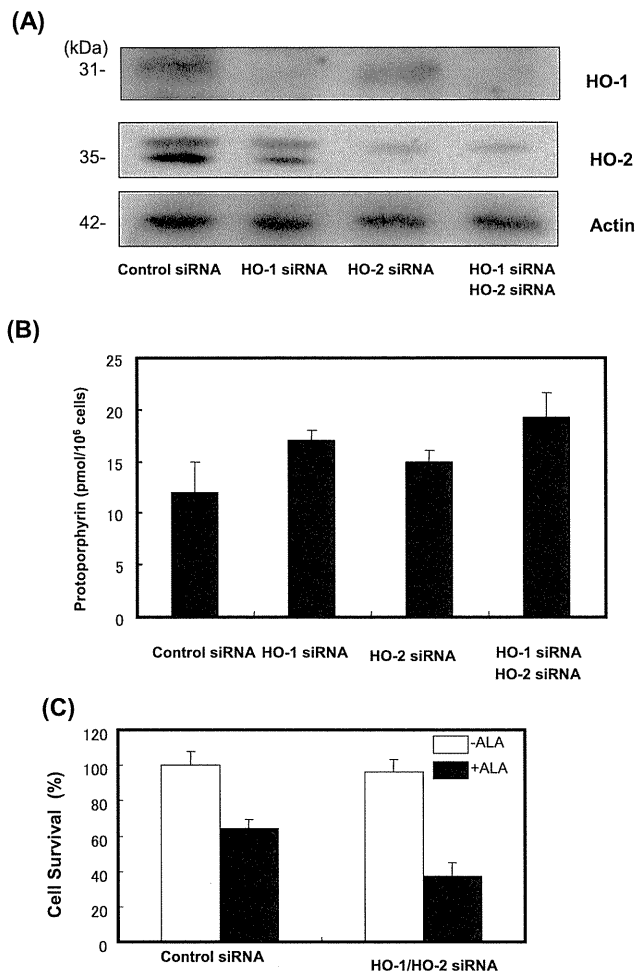


Figure 4. Enhancement of the ALA-induced accumulation of protoporphyrin and photodamage by knockdown of HO-1 and HO-2. (A) The cells (5×10^5) transfected with HO-1 and HO-2 siRNAs were cultured for 48 h, followed by incubation with 1 mM ALA for 16 h. The cellular protein from the cells as above was analyzed by SDS-PAGE. Immunoblots of HO-1 and HO-2 were carried out; (B) Porphyrin was extracted and determined; (C) Effect of double knockdown of HO-1 and HO-2 on the photodamage. The cells treated with HO-1/-2 siRNAs in combination were irradiated. The survival of cells was examined by MTT assay. Data are the mean \pm SD of three to four independent experiments.

control (Fig. 6C). Without irradiation, virtually no photodamage was observed. These results indicated that the decrease of the supply of iron in mitochondria led to the enhancement of ALA-induced photodamage.

DISCUSSION

This study demonstrated that the increased expression of heme-biosynthetic enzymes, including PBGD, UROS and CPOX in HeLa cells increased the accumulation of ALA-induced protoporphyrin and photodamage. The increased expression of PPOX did not have any effect. In cells highly expressing FECH, the accumulation of protoporphyrin decreased, presumably due to insertion of ferrous ions into protoporphyrin, which was consistent with our previous findings (7,8) that the accumulation of protoporphyrin was inversely correlated with the expression of FECH. Recently,

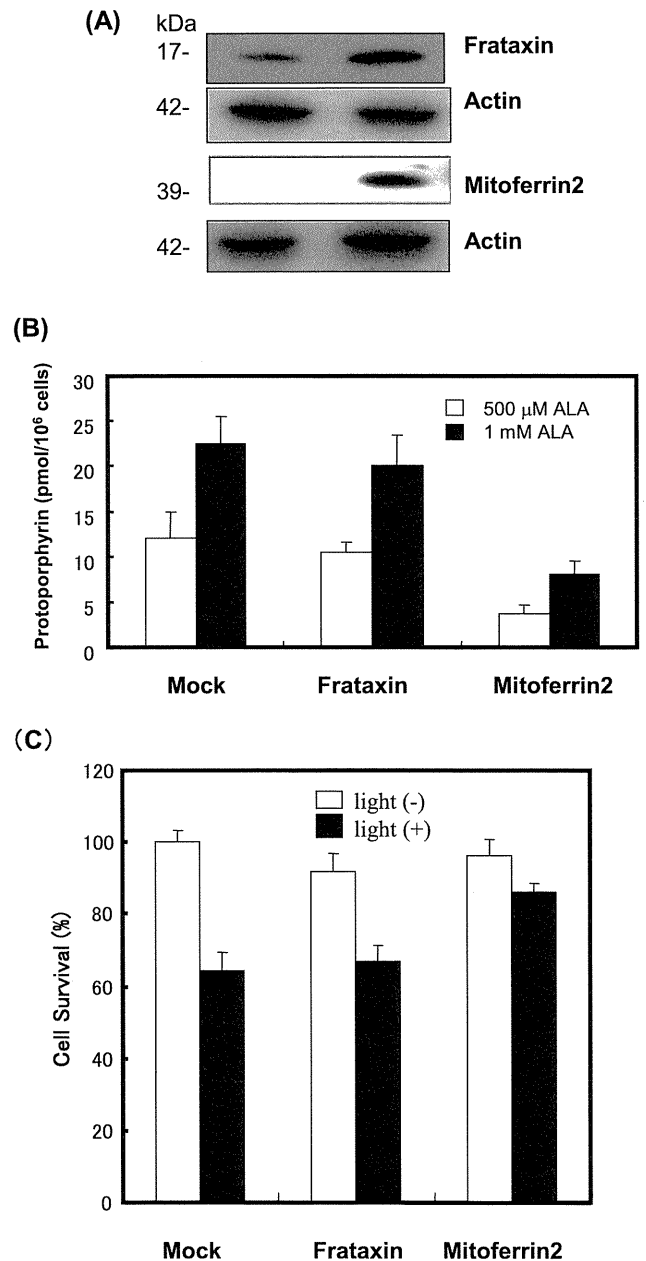


Figure 5. Effect of the expression of frataxin and mitoferrin-2 on the ALA-induced protoporphyrin and photodamage. HeLa cells (5×10^5) were transfected with pcDNA3-frataxin or pCG-C-mitoferrin-2 and incubated for 16 h. The cells were then incubated with 500 μ M and 1 mM ALA for 8 h. (A) Immunoblots. Cellular proteins from the cells as treated above were analyzed by SDS-PAGE, followed by immunoblotting with anti-frataxin and anti-HA, as the primary antibodies; (B) The porphyrin was extracted and measured; (C) Photodamage. The cells treated as above were irradiated. The survival of cells was examined by MTT assay. Data are the mean \pm SD of three to four independent experiments.

other investigators applied FECH siRNA to enhance ALA-PDT in glioma of septum and found a high efficacy of ALA-PDT *in vivo* (30). On the base of the fact that FECH deficiency leads to the accumulation of protoporphyrin leading to the inherited disease erythropoietic protoporphyria (31), the decrease of FECH activity is closely related to ALA-PDT. In addition to the decrease of FECH activity, it is reported that

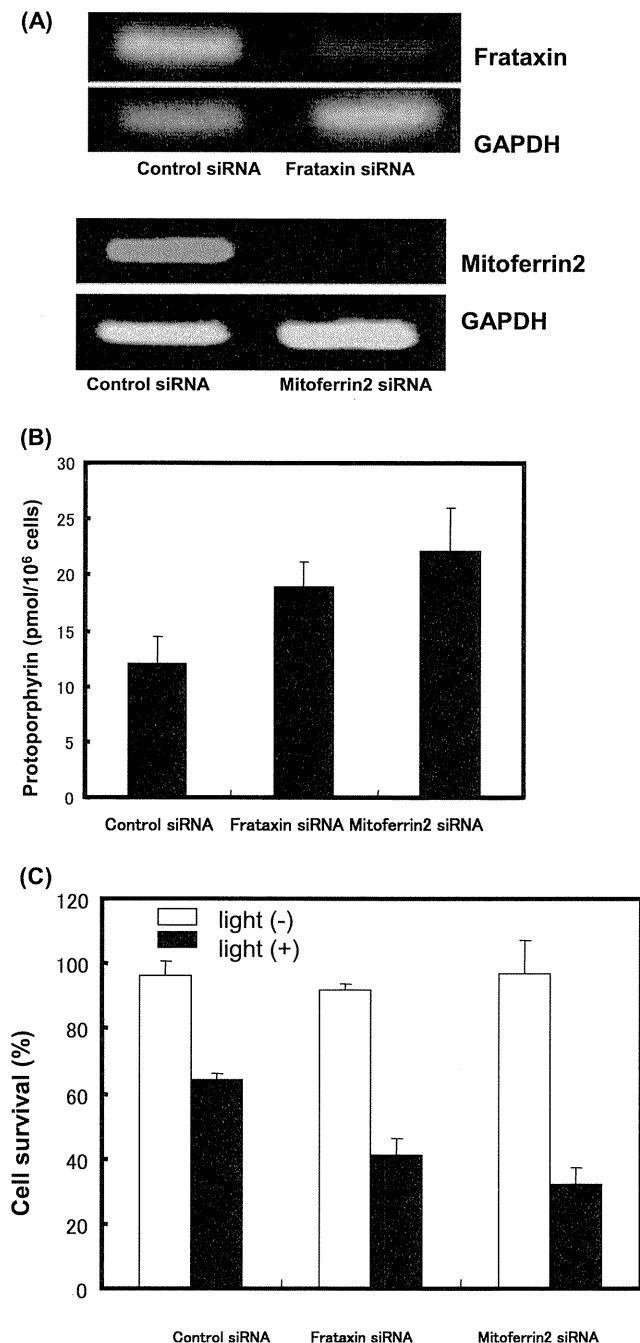


Figure 6. Enhancement of the ALA-induced accumulation of protoporphyrin and photodamage by knockdown of frataxin and mitoferrin-2. (A) The cells (5×10^5) transfected with frataxin or mitoferrin-2 siRNA were cultured for 48 h, followed by incubation with 1 mM ALA for 16 h. RNA was isolated from the cells treated as above. RT-PCR was performed to estimate the levels of frataxin and mitoferrin-2 mRNAs; (B) Porphyrin was extracted and determined; (C) Photodamage. The cells treated as above were irradiated. Surviving cells were examined by MTT assay. Data are the mean \pm SD of three independent experiments.

CPOX expression on ALA-PDT because the transfection of the cells with CPOX-expression plasmid caused an increase in the ALA-induced photodamage. Hinnen *et al.* (34) and Krieg *et al.* (35) reported that an increase in the expression of PBGD in adenocarcinoma cells was related to the hypersensitivity of ALA-PDT, suggesting that the elevation of PBGD in cancerous cells might be a useful parameter for predicting the accumulation of protoporphyrin. We found that the augmentation of PBGD expression caused an increase in the ALA-induced accumulation of protoporphyrin and photodamage. Thus, the elevation of the level of heme-biosynthetic enzymes, including PBGD, UROS and CPOX could be responsible for the high accumulation of protoporphyrin in tumor cells. In addition, considering that silencing of ALA-dehydratase caused the decrease of ALA-induced accumulation of protoporphyrin (36), ALA-dehydratase seems to play a role for ALA-PDT.

The results in our study supported the findings of previous studies that the supply of iron and the reuse of iron from heme by HO reduced the ALA-induced accumulation of protoporphyrin (27). Here, we demonstrated that the induction of HO-1 by hemin and heavy metal ions decreased the accumulation. It is possible that the decrease of the accumulation can be due to the heavy metal toxicity as the intoxication by heavy metal ions caused the reduction of ALA-induced accumulation of protoporphyrin (37). On the other hand, Sn-PP, an inhibitor of HO but not Co-PP, a substrate of HO, increased the ALA-induced accumulation of protoporphyrin (Fig. 2A). Furthermore, the expression of HO-1 in HeLa cells was shown to be inversely related to the ALA-induced accumulation of protoporphyrin (Fig. 3B). The increased expression of HO-2 also decreased the accumulation, and knockdown of the expression of HO-1/-2 in HeLa cells resulted in a marked enhancement of the photodamage (Fig. 4C). Thus, iron generated by HO-1 as well as HO-2 is reused for the iron-chelating reaction by FECH. As such, challenge of HO-1 and HO-2 siRNA may facilitate for the enhancement of ALA-PDT for tumors.

Some researchers (13) showed that the ALA-induced phototoxicity was variable among cancer cell lines even when knockdown of HO-1 in several cells by siRNA was carried out, and suggested that the level of HO-1 was unrelated to ALA-PDT. However, the contribution of HO-2 in ALA-PDT was not examined. We found that expression of HO-2 as well as HO-1 decreased the accumulation of protoporphyrin in the presence of ALA, whereas deficiency of HO-2 or HO-1 in HeLa cells increased the accumulation. In addition to the decreased expression of FECH in tumor cells, the low expression of HO-1/-2 in cancer cells may be linked to hyperphotosensitivity derived from ALA. Therefore, the decrease of HO function can cause the ALA-induced accumulation of protoporphyrin. Alternatively, we have shown that HO-1 is markedly induced not only by chemicals that produce oxidative stress involving the generation of reactive oxygen species but also by the substrate heme (28,29), and that HO-1 in ALA-treated cells was induced in time- and dose-dependent manners, and the induction of HO-1 was seen in the protoporphyrin-accumulated cells (8). It is considered that uncommitted heme in the cells is very dangerous for the maintenance of living systems, and reutilization of iron, including degradation of heme, catalyzed by HO, is essential for the homeostasis of iron in cells (9). By the treatment of cells

the treatment of prostate cancer cells with methotrexate, an anticancer reagent, resulted in an increase in ALA-induced PDT with concomitant elevation of CPOX (32). Sinha *et al.* (33) reported that up-regulation of CPOX enhanced ALA-PDT of prostate cancer cells. Our results support this effect of

with ALA, excess heme produced from ALA may induce HO-1. It was also possible that the accumulated protoporphyrin generates reactive oxygen species *via* autoxidation (38), which leads to the induction of HO-1. On the basis of the fact that HO degrades heme, producing iron, CO and biliverdin (12), the supply of iron for its reutilization reduced the protoporphyrin and high level of HO-1 in tumor cells may be responsible for their resistance to anticancer treatment. In contrast, the iron supply was stopped by the inhibition of the HO reaction with Sn-PP, leading to an increase in the production of protoporphyrin. The photosensitivity caused by the ALA-dependent accumulation of protoporphyrin was different among tumor cells. One of the reasons to explain the different photosensitivity may be the different rates for the production of heme and the degradation of heme in species of tumor cells.

It is well known that iron metabolism in mitochondria is different between normal and cancerous cells. Among molecules involved in mitochondrial iron metabolism, mitoferrin-2 functions in the import of mitochondrial iron in nonerythroid cells (16). Reduction of mitoferrin-1/2 levels by RNA interference resulted in the decrease of mitochondrial iron and heme synthesis (16). Mutation of erythroid-type mitoferrin in zebrafish caused defects in hemoglobinization (16). The present data revealed that knockdown of mitoferrin-2 in HeLa cells led to the increase in the ALA-induced accumulation of protoporphyrin and enhancement of photodamage. On the other hand, transient expression of mitoferrin-2 in HeLa cells decreased the ALA-induced accumulation of protoporphyrin, which showed the increased availability of iron for the reaction of FECH. Although no study on whether the expression of mitoferrin-2 in cancerous cells is reduced has been reported, it is possible that the function of mitoferrin-2 can be impaired in transformed cells.

The overexpression of mitochondrial frataxin in cancer cells decreased ROS production and induced mitochondrial functions, including respiratory, membrane potential and ATP content (39). It is reported that several cancer cells do not express detectable frataxin, but untransformed cells produce frataxin (40). Thus, the reduction of the function of frataxin in cancerous cells lead to the decrease of mitochondrial function and may contribute to enhancement of cancer-specific ALA-PDT. HeLa cells used in this study produced detectable frataxin and transient overexpression of frataxin did not affect ALA-induced accumulation of protoporphyrin, suggesting that the expression of frataxin in control HeLa cells can be enough to maintain iron metabolism in mitochondria. The expression of frataxin in frataxin-deficient tumor cells may reduce ALA-PDT. On the other hand, knockdown of frataxin led to an increase in the ALA-induced photodamage with the accumulation of protoporphyrin. Frataxin is an iron-chaperon and plays an essential role in Fe-S cluster biogenesis in mitochondria (39). Considering that FECH is an Fe-S cluster-containing protein and the expression level of FECH is dependent on the intracellular level of iron (41), a loss of function of frataxin decreases the level of FECH, leading to enhancement of ALA-PDT. In contrast, Schoenfeld *et al.* (17) reported that lymphoblasts of frataxin-knockout mice were protected from ALA-induced phototoxicity by the reduced expression of CPOX. The different effect of frataxin deficiency on ALA-induced photodamage can be due to different

metabolic regulations of mitochondrial iron utilization between normal and cancerous cells. Thus, the present study revealed important roles of multiple factors such as porphyrin synthesis, iron reutilization and mitochondrial iron metabolism for characteristics of tumor-specific ALA-dependent accumulation of protoporphyrin. Further systematic studies should shed light on the mechanism of resistance against PDT and overcome the limitation in clinical application for various carcinoma cells.

Acknowledgements—We thank Dr. S. Shibahara for kind gifts of pHHO-1 and pHHO-2. This study was supported in part by grants from the Ministry of Health, Labor and Welfare of Japan, and from the Ministry of Education, Science, Sports and Culture of Japan.

REFERENCES


- Dougherty, T. J., C. J. Gomer, B. W. Henderson, G. Jori, D. Kessel, M. Korbelik, J. Moan and Q. Peng (1998) Photodynamic therapy. *J. Natl. Cancer Inst.* **90**, 889–905.
- De Rosa, F. S., R. F. Lopez, J. A. Thomazine, A. C. Tedesco, N. Lange and M. Bentley (2004) *In vitro* metabolism of 5-ALA esters derivatives in hairless mice skin homogenate and *in vivo* PpIX accumulation studies. *Pharm. Res.* **21**, 2247–2252.
- Fischer, F., E. F. Dickson, J. C. Kennedy and R. H. Pottier (2001) An affordable, portable fluorescence imaging device for skin lesion detection using a dual wavelength approach for image contrast enhancement and aminolaevulinic acid-induced protoporphyrin IX. Part II. *In vivo* testing. *Lasers Med. Sci.* **16**, 207–212.
- Fischer, F., E. F. Dickson, R. H. Pottier and H. Wieland (2001) An affordable, portable fluorescence imaging device for skin lesion detection using a dual wavelength approach for image contrast enhancement and aminolaevulinic acid-induced protoporphyrin IX. Part I. Design, spectral and spatial characteristics. *Lasers Med. Sci.* **16**, 199–206.
- Hirschberg, H., F. A. Uzal, D. Chighvinadze, M. J. Zhang, Q. Peng and S. J. Madsen (2008) Disruption of the blood-brain barrier following ALA-mediated photodynamic therapy. *Lasers Surg. Med.* **40**, 535–542.
- Furuyama, K., K. Kaneko and P. D. Vargas (2007) Heme as a magnificent molecule with multiple missions: heme determines its own fate and governs cellular homeostasis. *Tohoku J. Exp. Med.* **213**, 1–16.
- Yamamoto, F., Y. Ohgari, N. Yamaki, S. Kitajima, O. Shimokawa, H. Matsui and S. Taketani (2007) The role of nitric oxide in delta-aminolevulinic acid (ALA)-induced photosensitivity of cancerous cells. *Biochem. Biophys. Res. Commun.* **353**, 541–546.
- Ohgari, Y., Y. Nakayasu, S. Kitajima, M. Sawamoto, H. Mori, O. Shimokawa, H. Matsui and S. Taketani (2005) Mechanisms involved in delta-aminolevulinic acid (ALA)-induced photosensitivity of tumor cells: relation of ferrochelatase and uptake of ALA to the accumulation of protoporphyrin. *Biochem. Pharmacol.* **71**, 42–49.
- Taketani, S. (2005) Acquisition, mobilization and utilization of cellular iron and heme: endless findings and growing evidence of tight regulation. *Tohoku J. Exp. Med.* **205**, 297–318.
- Andoh, Y., H. Suzuki, M. Araki, A. Mizutani, T. Ohashi, T. Okumura, Y. Adachi, S. Ikehara and S. Taketani (2004) Low- and high-level expressions of heme oxygenase-1 in cultured cells under uninduced conditions. *Biochem. Biophys. Res. Commun.* **320**, 722–729.
- Ryter, S. W. and A. M. Choi (2009) Heme oxygenase-1/carbon monoxide: from metabolism to molecular therapy. *Am. J. Respir. Cell Mol. Biol.* **41**, 251–260.
- Jansen, T., M. Hortmann, M. Oelze, B. Opitz, S. Steven, R. Schell, M. Knorr, S. Karbach, S. Schuhmacher, P. Wenzel, T. Münzel and A. Daiber (2010) Conversion of biliverdin to bilirubin by biliverdin reductase contributes to endothelial cell protection by heme oxygenase-1-evidence for direct and indirect antioxidant actions of bilirubin. *J. Mol. Cell. Cardiol.* **49**, 186–195.

13. Miyake, M., M. Ishii, K. Kawashima, T. Kodama, K. Sugano, K. Fujimoto and Y. Hirao (2009) siRNA-mediated knockdown of the heme synthesis and degradation pathways: modulation of treatment effect of 5-aminolevulinic acid-based photodynamic therapy in urothelial cancer cell lines. *Photochem. Photobiol.* **85**, 1020–1027.
14. Frank, J., M. R. Lornejad-Schäfer, H. Schöffl, A. Flaccus, C. Lambert and H. K. Biesalski (2007) Inhibition of heme oxygenase-1 increases responsiveness of melanoma cells to ALA-based photodynamic therapy. *Int. J. Oncol.* **31**, 1539–1545.
15. Modica-Napolitano, J. S., M. Kulawiec and K. K. Singh (2007) Mitochondria and human cancer. *Curr. Mol. Med.* **7**, 121–131.
16. Paradkar, P. N., K. B. Zumbrennen, B. H. Paw, D. M. Ward and J. Kaplan (2009) Regulation of mitochondrial iron import through differential turnover of mitoferrin 1 and mitoferrin 2. *Mol. Cell. Biol.* **29**, 1007–1016.
17. Schoenfeld, R. A., E. Napoli, A. Wong, S. Zhan, L. Reutenauer, D. Morin, A. R. Buckpitt, F. Taroni, B. Lonnerdal, M. Ristow, H. Puccio and G. A. Cortopassi (2005) Frataxin deficiency alters heme pathway transcripts and decreases mitochondrial heme metabolites in mammalian cells. *Hum. Mol. Genet.* **15**, 3787–3799.
18. Thierbach, R., T. J. Schulz, F. Isken, A. Voigt, B. Mietzner, G. Drewes, J. C. von Kleist-Retzow, R. J. Wiesner, M. A. Magnuson, H. Puccio, A. F. Pfeiffer, P. Steinberg and M. Ristow (2005) Targeted disruption of hepatic frataxin expression causes impaired mitochondrial function, decreased life span and tumor growth in mice. *Hum. Mol. Genet.* **14**, 3857–3864.
19. Inoue, K., T. Karashima, M. Kamada, T. Shuin, A. Kurabayashi, M. Furihata, H. Fujita, K. Utsumi and J. Sasaki (2009) Regulation of 5-aminolevulinic acid-mediated protoporphyrin IX accumulation in human urothelial carcinomas. *Pathobiology* **76**, 303–314.
20. Choudry, K., R. C. Brooke, W. Farrar and L. E. Rhodes (2003) The effect of an iron chelating agent on protoporphyrin IX levels and phototoxicity in topical 5-aminolevulinic acid photodynamic therapy. *Br. J. Dermatol.* **149**, 124–130.
21. Taketani, S., T. Furukawa and K. Furuyama (2001) Expression of coproporphyrinogen oxidase and synthesis of hemoglobin in human erythroleukemia K562 cells. *Eur. J. Biochem.* **268**, 1705–1711.
22. Nishimura, K., S. Taketani and H. Inokuchi (1995) Cloning of a human cDNA for protoporphyrinogen oxidase by complementation *in vivo* of a hemG mutant of *Escherichia coli*. *J. Biol. Chem.* **270**, 8076–8080.
23. Vargas, P. D., K. Furuyama, S. Sassa and S. Shibahara (2008) Hypoxia decreases the expression of the two enzymes responsible for producing linear and cyclic tetrapyrroles in the heme biosynthetic pathway. *FEBS J.* **275**, 5947–5959.
24. Yoshida, T., P. Biro, T. Cohen, R. M. Müller and S. Shibahara (1988) Human heme oxygenase cDNA and induction of its mRNA by hemin. *Eur. J. Biochem.* **171**, 457–461.
25. Shibahara, S., M. Yoshizawa, H. Suzuki, K. Takeda, K. Meguro and K. Endo (1993) Functional analysis of cDNAs for two types of human heme oxygenase and evidence for their separate regulation. *J. Biochem.* **113**, 214–218.
26. Sakaino, M., T. Kataoka and S. Taketani (2009) Post-transcriptional regulation of the expression of ferrochelatase by its variant mRNA. *J. Biochem.* **145**, 733–738.
27. Ohgari, Y., Y. Miyata, T. T. Chau, S. Kitajima, Y. Adachi and S. Taketani (2011) Quinolone compounds enhance delta-aminolevulinic acid-induced accumulation of protoporphyrin IX and photosensitivity of tumour cells. *J. Biochem.* **149**, 153–160.
28. Masuya, Y., K. Hioki, R. Tokunaga and S. Taketani (1998) Involvement of the tyrosine phosphorylation pathway in induction of human heme oxygenase-1 by hemin, sodium arsenite, and cadmium chloride. *J. Biochem.* **124**, 628–633.
29. Harada, H., R. Sugimoto, A. Watanabe, S. Taketani, K. Okada, E. Warabi, R. Siow, K. Itoh, M. Yamamoto and T. Ishii (2008) Differential roles for Nrf2 and AP-1 in upregulation of HO-1 expression by arsenite in murine embryonic fibroblasts. *Free Radic. Res.* **42**, 297–304.
30. Teng, L., M. Nakada, S. G. Zhao, Y. Endo, N. Furuyama, E. Nambu, I. V. Pyko, Y. Hayashi and J. I. Hamada (2011) Silencing of ferrochelatase enhances 5-aminolevulinic acid-based fluorescence and photodynamic therapy efficacy. *Br. J. Cancer* **104**, 798–807.
31. Yasui, Y., S. Muranaka, T. Tahara, R. Shimizu, S. Watanabe, Y. Horie, E. Nanba, H. Uezato, A. Takamiyagi, S. Taketani and R. Akagi (2002) A new ferrochelatase mutation combined with low expression alleles in a Japanese patient with erythropoietic protoporphyria. *Clin. Sci. (Lond.)* **102**, 501–506.
32. Anand, S., G. Honari, T. Hasan, P. Elson and E. V. Maytin (2009) Low-dose methotrexate enhances aminolevulinic acid-based photodynamic therapy in skin carcinoma cells *in vitro* and *in vivo*. *Clin. Cancer Res.* **15**, 3333–3343.
33. Sinha, A. K., S. Anand, B. J. Ortel, Y. Chang, Z. Mai, T. Hasan and E. V. Maytin (2006) Methotrexate used in combination with aminolevulinic acid for photodynamic killing of prostate cancer cells. *Br. J. Cancer* **95**, 485–495.
34. Hinnen, P., F. W. de Rooij, E. M. Terlou, A. Edixhoven, H. van Dekken, R. van Hillegersberg, H. W. Tilanus, J. H. Wilson and P. D. Siersema (2000) Porphyrin biosynthesis in human Barrett's oesophagus and adenocarcinoma after ingestion of 5-aminolevulinic acid. *Br. J. Cancer* **83**, 539–543.
35. Krieg, R. C., H. Messmann, J. Rauch, S. Seeger and R. Knuechel (2002) Metabolic characterization of tumor cell-specific protoporphyrin IX accumulation after exposure to 5-aminolevulinic acid in human colonic cells. *Photochem. Photobiol.* **76**, 518–525.
36. Grinblat, B., N. Pour and Z. Malik (2006) Regulation of porphyrin synthesis and photodynamic therapy in heavy metal intoxication. *J. Environ. Pathol. Toxicol. Oncol.* **25**, 145–158.
37. Feuerstein, T., A. Schauder and Z. Malik (2009) Silencing of ALA dehydratase affects ALA-photodynamic therapy efficacy in K562 erythroleukemic cells. *Photochem. Photobiol. Sci.* **8**, 1461–1466.
38. Krieg, R. C., S. Fickweiler, O. S. Wolfbeis and R. Knuechel (2000) Cell-type specific protoporphyrin IX metabolism in human bladder cancer *in vitro*. *Photochem. Photobiol.* **72**, 226–233.
39. Stemmler, T. L., E. Lesuisse, D. Pain and A. Dancis (2010) Frataxin and mitochondrial FeS cluster biogenesis. *J. Biol. Chem.* **285**, 26737–26743.
40. Schulz, T. J., R. Thierbach, A. Voigt, G. Drewes, B. Mietzner, P. Steinberg, A. F. Pfeiffer and M. Ristow (2006) Induction of oxidative metabolism by mitochondrial frataxin inhibits cancer growth: Otto Warburg revisited. *J. Biol. Chem.* **281**, 977–978.
41. Taketani, S., Y. Adachi and Y. Nakahashi (2000) Regulation of the expression of human ferrochelatase by intracellular iron levels. *Eur. J. Biochem.* **267**, 4685–4692.

Ferrochelatase Catalyzes the Formation of Zn-protoporphyrin of Dry-Cured Ham via the Conversion Reaction from Heme in Meat

Tuan Thanh Chau,[†] Mutsumi Ishigaki,[†] Takao Kataoka,[†] and Shigeru Taketani^{*,†,‡}

[†]Department of Biotechnology and [‡]Insect Biomedical Center, Kyoto Institute of Technology, Kyoto 606-8585, Japan

 Supporting Information

ABSTRACT: Ferrochelatase (FECH), the enzyme at the last step of the heme-biosynthetic pathway, is involved in the formation of Zn-protoporphyrin via an iron-removal reaction of heme. To improve the efficacy of the formation of Zn-protoporphyrin from heme, the use of recombinant FECHs from porcine, yeast, and bacteria was examined. Incubation of FECH with myoglobin in the presence of ascorbic acid and cysteine resulted in the efficient conversion of myoglobin-heme to Zn-protoporphyrin. Exogenously added recombinant yeast FECH facilitates the production of Zn-protoporphyrin from myoglobin-heme and heme in meat, via the replacement of iron in the protoporphyrin ring by zinc ions. A large amount of Zn-protoporphyrin was also generated by the catalysis of FECH using an intact piece of meat as a substrate. These findings can open up possible approaches for the generation of a nontoxic bright pigment, Zn-protoporphyrin, to shorten the incubation time required to produce dry-cured ham.

KEYWORDS: Ferrochelatase, Zn-protoporphyrin, conversion reaction, ham pigment, dry-cured ham

INTRODUCTION

In cooked ham, the red pigment, nitrosomyoglobin, is a result of thermal treatment of meat with nitrite.^{1,2} Because nitrosamines generated in nitrite-meat products are associated with a cancer risk,² nitrite-free or green ham has been a preferred alternative. Dry-cured ham (Parma ham), nitrite-free ham, is produced by the incubation of meat with sea salt for a long period at suitable temperature and humidity.³ Zn-protoporphyrin as a replacement product of protoheme (Fe-protoporphyrin)^{4,5} has been isolated as the main component of red pigments of these types of ham. Because of its safe and stable properties,^{6–8} Zn-protoporphyrin was the preferred replacement for nitrosomyoglobin. However, it is hard to develop the red pigment rapidly in meat products, and the formation of Zn-protoporphyrin in meat is not well understood.

Ferrochelatase (FECH) (EC 4.99.1.1), located at the inner membrane of the mitochondria in mammalian cells, catalyzes the insertion of ferrous ions into protoporphyrin IX to form protoheme.⁹ The gene for FECH has been isolated from various organisms, and the structures of FECH protein from bacteria to higher eukaryotes were found to be conserved. Mammalian FECH contains an iron–sulfur cluster at the carboxyl terminal of the protein,¹⁰ whereas most fungal and bacterial FECHs do not.^{5,10} The function of the cluster in the mammalian enzyme is unclear. Ferrous ions are the preferable targeting substrate of the enzyme to form heme in vivo.⁹ Furthermore, other corresponding metalloporphyrins can be produced via the enzyme catalysis of divalent metal ions including zinc, cobalt and nickel with porphyrin compounds in vitro. Although it was considered that FECH irreversibly catalyzes the insertion of metal ions into porphyrin ring, we showed that FECH can also catalyze the iron-removal (reverse) reaction from heme to create protoporphyrin in vivo and in vitro and the subsequent conversion reaction from heme to Zn-protoporphyrin in vitro.^{11,12} The iron-removal

reaction seems to be carefully controlled in vivo,¹¹ but the reaction could occur in vitro. Furthermore, the reaction of NADH-cytochrome *b*₅ reductase (metmyoglobin reductase) reduces the ferric ions in heme to ferrous ions, which leads to the conversion of hemin to Zn-protoporphyrin.

The formation of Zn-protoporphyrin in dry-cured ham is unclear. Several findings showed that bacteria in porcine meat were the main cause of the stable pigments during Parma ham processing.⁸ Recently, endogenous enzymes including FECH in meat have been identified as a potential cause of the pigment formation.^{11–16} Several compounds such as salt, ascorbic acid, and dithiothreitol can increase the formation of Zn-protoporphyrin to some extent.^{17–19} It is possible that the formation of Zn-protoporphyrin could occur via two pathways. First, an intermediate porphyrin, protoporphyrinogen, is oxidized by protoporphyrinogen oxidase to form protoporphyrin aerobically; then, Zn-protoporphyrin is produced by the insertion of zinc, which is present in large amounts in meat,²⁰ into the protoporphyrin.²¹ The other pathway, also identified in our findings, is that Zn-protoporphyrin is generated via the conversion reaction of heme, in which zinc is inserted into protoporphyrin as a product of the iron-removal reaction of heme in hemoproteins catalyzed by FECH.^{11,12,16} In this case, the replacement does not occur easily, especially in porcine muscle (meat). FECH from porcine muscle mitochondria catalyzes the insertion reaction of zinc into protoporphyrin to form Zn-protoporphyrin^{12,13,15} as well as the iron-removal reaction of heme, strongly suggesting that FECH acts as a conversion enzyme in porcine meat. However, the mechanism of Zn-protoporphyrin in hams is still speculative.

Received: August 5, 2011

Accepted: October 17, 2011

Revised: October 12, 2011

Published: October 17, 2011

To obtain the highly efficient conversion from myoglobin-heme and heme in meat to Zn-protoporphyrin, we tried to use the recombinant porcine and yeast FECH for the reaction. We here demonstrate that the recombinant enzyme is effective for the production of Zn-protoporphyrin. We also found the roles of reducing agents, such as ascorbic acid and cysteine, in enhancing the iron removal and conversion from heme to Zn-protoporphyrin under anaerobic conditions. Furthermore, the addition of recombinant yeast FECH into intact piece of raw meat is applied to facilitate the generation of Zn-protoporphyrin. These results may open up new methods to generate the natural red pigment of meat and could help to shorten the incubation period of dry-cured ham.

MATERIALS AND METHODS

Materials. The genomic DNA of the thermophilic bacterium *Thermus thermophilus* (NC_006461) was obtained from Japan Gene Bank. Mesoporphyrin IX, protoporphyrin IX, and Zn-protoporphyrin IX were from Frontier Scientific (Logan, UT). Horse hemoglobin (Hb) and myoglobin (Mb) were products of Sigma Co. (St. Louis, MO). Porcine muscles were generously donated by Itoh Ham Inc. (Moriya, Japan). Restriction endonuclease was obtained from Takara Co. (Tokyo, Japan). The other chemicals used were of analytical grade.

Recombinant Enzymes. Mouse NADH-cytochrome b_5 reductase and porcine FECH carrying His-tag were prepared as described previously.^{11,12} The FECH genes of *S. cerevisiae* and *T. thermophilus* were isolated by polymerase chain reaction (PCR) using corresponding genomic DNA. The primers used for yeast FECH were 5'-AAG GAT CCC GTC CTC ATG GCC TA-3' (forward) and 5'-AAG AAT TCT ATC TCG GCC ACG CCG C-3' (reverse), and those for *T. thermophilus* were 5'-AAG AAT TCG AAT GCA CAA AAG AGA T-3' (forward) and 5'-AAA AGC TTT CAA GTA GAT TCG TGA T-3' (reverse). The DNAs obtained were inserted into pET vector and transformed into *E. coli* BL21 strain. The bacteria were grown in LB medium for 16 h, and then, the culture medium was diluted by 10-fold in fresh LB medium. These enzymes were expressed with 0.3 mM isopropyl- β thiogalactopyranoside at 30 °C for 2 h. The cells were harvested by centrifugation and suspended in 20 mM Tris-HCl (pH 8.0), 10% glycerol, 1 mM dithiothreitol (DTT), 0.1% Tween 20, 20 mM imidazole, and 0.3 M NaCl, disrupted by sonication, and centrifuged at 500g at 4 °C for 10 min. The supernatants were shaken with Ni²⁺-NTA beads (Qiagen, Valencia, CA) and washed three times with the above solution. The enzymes were eluted with 20 mM Tris-HCl (pH 8.0), 10% glycerol, 0.1% Tween 20, 0.25 M imidazole, 1 mM DTT, and 0.3 M NaCl. The protein concentration was measured by the method of Lowry et al.²² or Bradford,²³ using bovine serum albumin as the standard.

Electrophoresis of FECH. The proteins were analyzed by sodium dodecyl sulfate–polyacrylamide gel electrophoresis (SDS-PAGE) and stained with Coomassie Brilliant Blue (CBB) as described previously.¹²

Enzyme Assay. The FECH activity (forward reaction) was determined by measuring the insertion of zinc into mesoporphyrin, as described previously.²⁴ For measuring the iron-removal activity of FECH, a reaction mixture containing 1 mg of horse hemoglobin or myoglobin, 6 mM ascorbic acid, and 10 mM potassium phosphate buffer (pH 6.5) in a total volume of 1.0 mL was used in a Thurburg vacuum tube.²⁵ The dissolved gas was removed in vacuo and replaced by nitrogen. The reaction was carried out at 30 °C for 24 h. To examine the conversion of heme to Zn-protoporphyrin, 0.1 mM zinc ion was added to the reaction mixture.¹¹ The conversion from heme in meat to Zn-protoporphyrin was carried out as described above, except that hemoproteins were replaced by 1.0–15 g of porcine muscle (meat). Gas in the reaction tubes was removed as above and replaced with nitrogen.

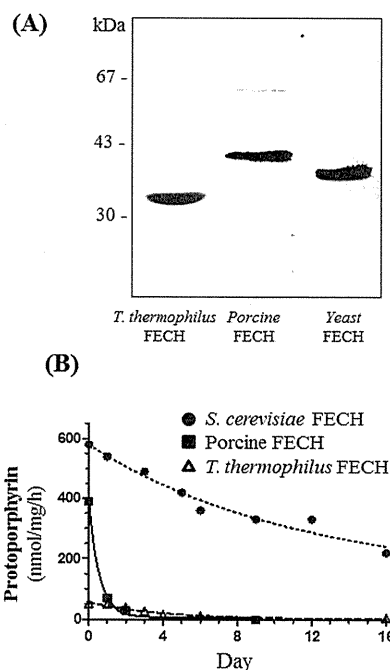


Figure 1. Characterization of the iron-removal activity and conversion reaction of porcine, yeast, and thermophilic bacterial FECH. (A) SDS-PAGE of purified porcine FECH (42 kDa), *T. thermophilus* FECH (33 kDa), and yeast FECH (39 kDa). The recombinant porcine, yeast, and thermophilic bacterial FECHs were expressed in *E. coli* and purified. One microgram of purified enzyme was analyzed by SDS-PAGE and stained using Coomassie Brilliant Blue. (B) The stability of porcine, yeast, and thermophilic bacterial FECH. The purified recombinant enzymes in 20 mM Tris-HCl (pH 8.0) containing 0.3 M NaCl were stored at 18 °C for the indicated period, and the iron-removal reaction was examined. Data are expressed as means \pm SDs of triplicate experiments.

Oxygen was further absorbed with a packet of AnaeroPack for Cell, disposable oxygen, and carbon dioxide-generating agent (Mitsubishi Gas Chemical Co., Tokyo, Japan). The reaction was carried out at 30 °C for 24 h.

Analysis of Metalloporphyrin and Porphyrin Pigments.

Zn-protoporphyrin and protoporphyrin were extracted with acetone/ethanol (1:1 v/v) and determined by fluorospectrophotometry from 550 to 670 nm (Zn-protoporphyrin) or 600 to 700 nm (protoporphyrin) with an excitation of 400 nm (Figure S1).¹² Heme in the reaction mixture or porcine muscle was determined by the reduced–oxidized difference spectrum of pyridine hemochromogen¹¹ after extraction with ethyl acetate/acetic acid (3:1; v/v).

Photoimage. The extracts of the reaction mixture after incubation were transferred to quartz cuvettes and exposed to 360 nm UV light in a dark room at room temperature. A photograph of the emerged color was taken with focal ration, $f/2.5$, time of exposure, $t = 1$ s, and film speed, ISO = 200.

Statistical Analysis. Results were shown as means \pm standard deviations (SDs) and analyzed using unpaired Student's t test. All statistical analyses were calculated significant at level of $p < 0.05$ using GraphPad Prism software version 5.02 (GraphPad Software, Inc., CA).

RESULTS

Characterization of Yeast FECH in the Conversion of Hemoproteins to Zn-protoporphyrin. We^{11,12} previously reported that porcine FECH catalyzes the iron removal from heme

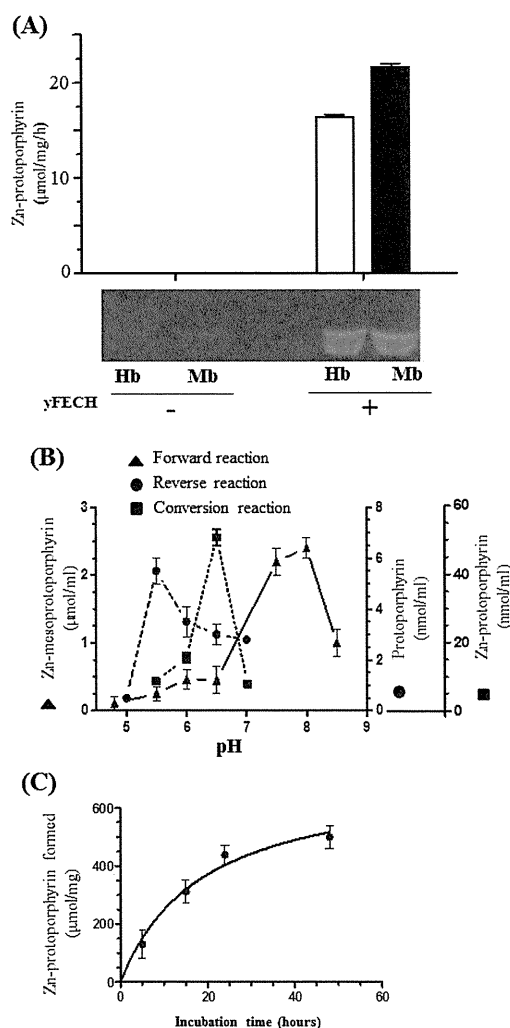


Figure 2. Kinetic study of yeast FECH. (A) The formation of Zn-protoporphyrin from hemoproteins. The reaction mixture (1.0 mL) contained 1 mg/mL myoglobin or 1 mg/mL hemoglobin, 6 mM ascorbic acid, 0.2 mM zinc acetate, and 0.3 μg of yeast FECH, in 10 mM potassium phosphate buffer, pH 6.5. The reaction was carried out at 30 °C for 24 h, and the formation of Zn-protoporphyrin was measured (upper panel). The ethanol/acetone extracts in the cuvettes were exposed to UV light in a dark room. The fluorescent image after the reaction was observed (lower panel), and the red color shows the production of Zn-protoporphyrin. (B) Effect of pH. The reactions were performed under the conditions as described above, except for the use of 10 mM potassium phosphate buffer with indicated pH. (C) Time course on the formation of Zn-protoporphyrin from myoglobin. The reactions were performed as described above, except that the incubation period was varied. Data are expressed as means ± SDs of 2–4 independent experiments.

as well as the conversion of heme to Zn-protoporphyrin and suggested that a large amount of Zn-protoporphyrin in Parma ham may be generated via iron-removal and conversion reactions of FECH from myoglobin-heme. However, the reaction was not fully identified, and the porcine enzyme only produced a small amount of Zn-protoporphyrin from hemin.¹² Thus, we tried to improve conditions to obtain a high yield of Zn-protoporphyrin from myoglobin by FECH. First, we searched for FECH from other sources because the reverse and conversion activities using mammalian FECH were not high because of instability of

mammalian FECH. We cloned FECH genes from the bacterium *T. thermophilus* and the yeast *S. cerevisiae* and expressed them in *E. coli*. The recombinant enzymes were purified using a nickel column and analyzed by 10% SDS-PAGE. The molecular masses of porcine, yeast, and bacterial FECH were 42, 39, and 33 kDa, respectively (Figure 1A). We then compared the iron removal (reverse activity) and stability of the enzymes (Figure 1B). When the enzymes were freshly prepared, the strongest activity was obtained with yeast enzyme. Porcine enzyme showed two-thirds of the activity of the yeast enzyme, and the bacterial one showed the lowest activity. To compare the stability of the three enzymes, they in 20 mM Tris-HCl (pH 8.0) containing 0.3 M NaCl were stored at 18 °C for the indicated period, and then, the reverse activity was examined. Yeast FECH showed 42% of the initial activity after storage for half a month, corresponding to a half-life of the activity ($t_{0.5}$) of 12 days, whereas porcine FECH was unstable and showed $t_{0.5}$ of 12 h. When the yeast enzyme was stored at 4 °C for a month, virtually no loss of the activity was observed. The bacterial FECH showed lower activity although it was more stable than the porcine enzyme. Thus, the yeast FECH showed strong activity and was suitable to obtain a high yield of Zn-protoporphyrin. Figure 2A shows the formation of Zn-protoporphyrin with myoglobin and hemoglobin catalyzed by yeast FECH. A considerable amount of Zn-protoporphyrin was formed with 1 mg/mL myoglobin or hemoglobin, whereas no Zn-protoporphyrin was found in the reactions without FECH. After Zn-protoporphyrin in the extracts was determined, the extracts upon exposure to UV light showed strong red fluorescence (Figure 2A, lower panel). Thus, yeast FECH catalyzes the conversion reaction from hemoproteins to Zn-protoporphyrin. Although the forward reaction of FECH showed an optimum at pH 7.5–8.0, the reverse one did at pH 5.5 (Figure 2B), which was consistent with previous observations.¹² When the pH profile of the conversion reaction from hemoglobin to Zn-protoporphyrin was examined, the highest activity was obtained at pH 6.5.

Then, we examined the time course of the conversion reaction using myoglobin as a substrate. To protect the stability of FECH and hemoproteins, we selected the incubation temperature of 30 °C. The formation of Zn-protoporphyrin gradually increased with time and reached a plateau by 24 h of incubation (Figure 2C). Kinetic properties of the conversion reaction from myoglobin and Zn^{2+} were also determined. The enzyme showed a V_{max} value of about 30 μmol of Zn-protoporphyrin formed/mg of protein/h, and K_m values for Zn^{2+} and myoglobin were 60 (Figure S2A in the Supporting Information) and 12 μM (Figure S2B in the Supporting Information), respectively.

To remove iron from heme, the reduced heme in myoglobin is required.¹¹ Thus, we examined the effect of reductants on the promotion of the reaction. NADH-cytochrome b_5 reductase can maintain the reduced form of myoglobin. The addition of recombinant NADH-cytochrome b_5 reductase with NADH caused weak conversion activity. Ascorbic acid (6 mM) and cysteine (6 mM) as additives showed marked stimulation (Figure S3 in the Supporting Information). Glutathione (6 mM) showed a weak effect (data not shown). When the concentration of ascorbic acid was changed, the activity increased dependent on the concentration up to 6 mM and then decreased (Figure 3A). Cysteine at a high concentration was effective. It is known that pig leg is treated with salt powder at the first step of dry-cured ham processing.³ We thus examined whether NaCl affects the formation of Zn-protoporphyrin from myoglobin-heme. As

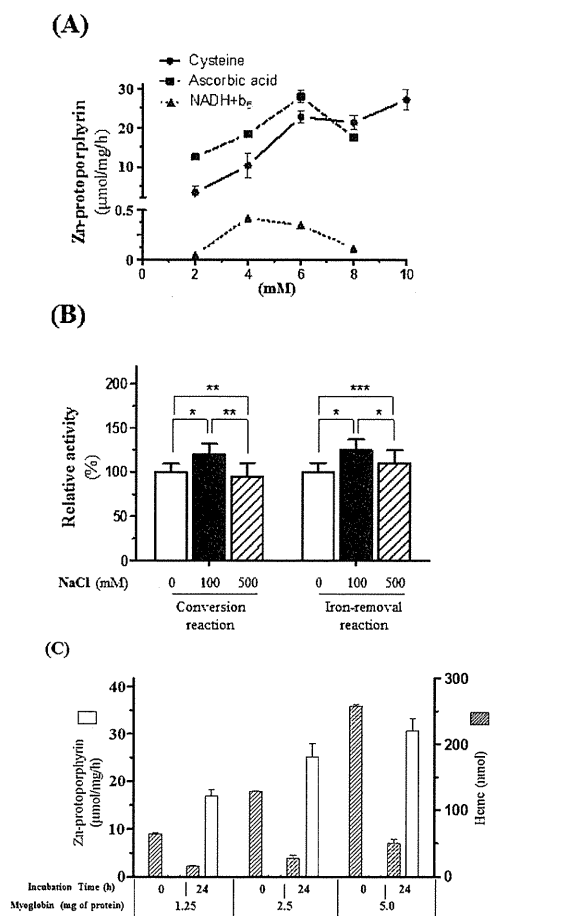


Figure 3. Formation of Zn-protoporphyrin of recombinant yeast FECH with myoglobin-heme or hemoglobin-heme. (A) Effect of reductants with yeast FECH on the conversion of myoglobin-heme to Zn-protoporphyrin. Yeast FECH was incubated in the reaction mixture similar to that described in the legend to Figure 2, except that the concentration of reductants was varied. NADH (2–8 mM) and mouse NADH-cytochrome *b*₅ reductase (10 µg of protein) for replacement of reductants were also used. (B) Effect of NaCl. The reaction was performed under the conditions as described above, except for the addition of the indicated concentration of NaCl. Data were tested the significant by using Student's *t* test, 0.05 < **p* < 0.1, 0.1 < ***p* < 0.5, and ****p* > 0.5. (C) Change in the proportion of Zn-protoporphyrin and myoglobin-heme by yeast FECH. The conversion reaction was performed similarly to the conditions as described above, except for the use of the indicated concentration of myoglobin. Protoporphyrin and Zn-protoporphyrin were examined by fluorospectrophotometry. Heme was determined using the reduced-oxidized pyridine hemochromogen. Data are expressed as means ± SDs of triplicate experiments.

shown in Figure 3B, the addition of NaCl at all concentrations did not show any significant statistical effect.

We next examined the change in the proportion of Zn-protoporphyrin to heme by the enzyme reaction. The amount of Zn-protoporphyrin increased after the incubation, which was accompanied by the decrease of heme (Figure 3C). At all examined concentrations of myoglobin, Zn-protoporphyrin was produced in a manner dependent on the initial concentration of myoglobin. It is evident that the conversion reaction of Zn-protoporphyrin from myoglobin-heme occurs via the catalysis of FECH.

Effect of Yeast FECH on the Conversion of Heme in Porcine Muscle (Meat) to Zn-protoporphyrin. We examined

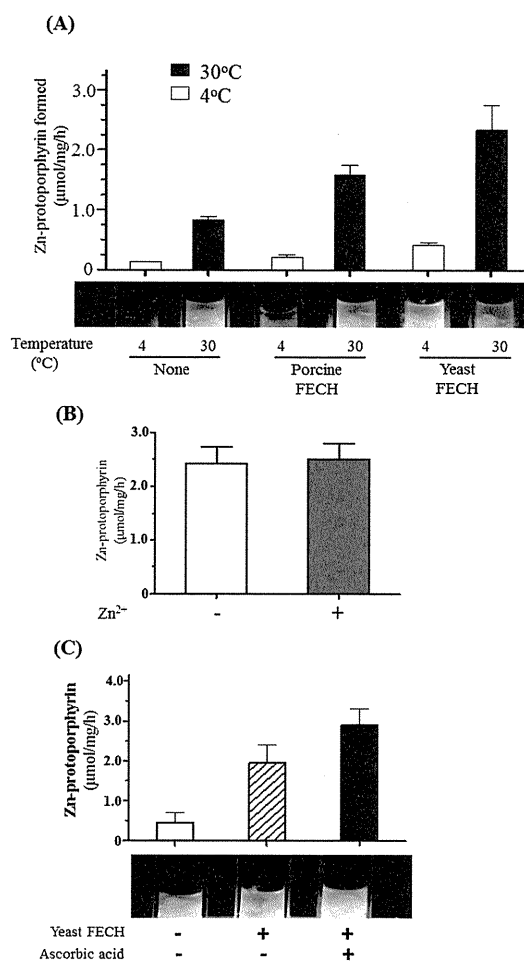


Figure 4. Conversion of heme in porcine muscle to Zn-protoporphyrin. (A) The reaction mixture containing porcine muscle (1 g wet weight) and 10 mM potassium phosphate buffer, pH 6.5, in the presence of porcine and yeast FECH (0.3 µg) was incubated at 4 or 30 °C for 24 h. The formation of Zn-protoporphyrin was measured (upper panel). Data are expressed as means ± SDs of triplicate experiments. The fluorescence in the ethanol/acetone extracts was observed (lower panel). (B) Effect of exogenous zinc ions on the conversion reaction. The reaction was performed under the conditions as described above, except for the addition of 0.2 mM zinc acetate. (C) Effect of ascorbic acid (upper panel). The incubation as above was carried out with or without 6 mM ascorbic acid. The lower panel shows a fluorescent image of the Zn-protoporphyrin (pink) produced.

the effect of FECH on the formation of Zn-protoporphyrin from heme in porcine muscle (meat). Meat (1 g) was added to the reaction mixture containing 6 mM ascorbic acid and porcine FECH or yeast FECH (0.3 µg). After anaerobic incubation at 4 or 30 °C for 24 h, the reaction mixtures with meat were homogenized, and porphyrins were extracted with ethanol/acetone (1:1, v/v). The results in Figure 4A (upper panel) revealed that the formation of Zn-protoporphyrin without recombinant FECH occurred at 30 °C. The yield of Zn-protoporphyrin with yeast enzyme was much higher than those without or with exogenous porcine FECH. The pink color corresponding to Zn-protoporphyrin by UV light was observed in the case of 30 °C incubation, and the intensity with recombinant FECH was stronger than that without FECH (lower panel). Using meat as a reaction source, the addition of zinc acetate to

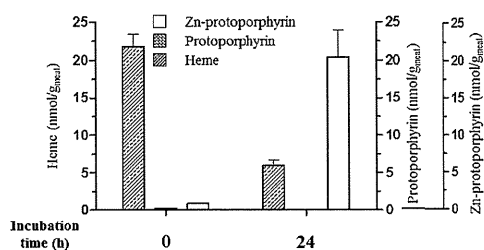


Figure 5. Proportion of metalloporphyrins and protoporphyrin in porcine muscle by the incubation with yeast FECH. The reaction mixture containing 1 g of meat (porcine muscle), 6 mM ascorbic acid, 0.3 μ g of yeast FECH, and 10 mM potassium phosphate buffer (pH 6.5) was incubated at 30 °C for 24 h. The contents of Zn-protoporphyrin, protoporphyrin, and heme were examined. Data are expressed as means \pm SDs of 2–4 independent experiments.

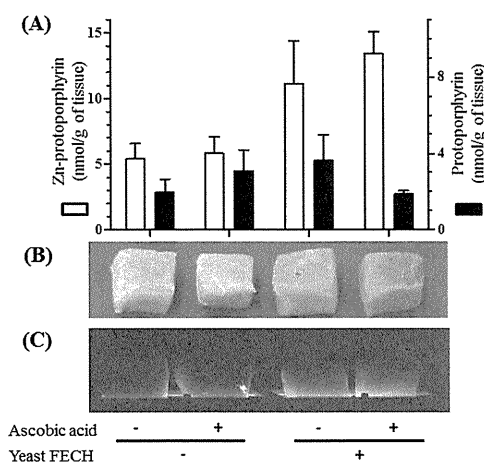


Figure 6. Conversion of heme in meat to Zn-protoporphyrin using the intact piece of porcine muscle. (A) The formation of Zn-protoporphyrin from heme in tissues of porcine muscle. The solution (1.0 mL) containing 1 μ g of yeast FECH, 6 mM ascorbic acid, and 10 mM potassium phosphate buffer, pH 6.5, was injected into porcine muscle (15 g). The meat was incubated anaerobically at 30 °C for 24 h. After incubation, Zn-protoporphyrin and protoporphyrin were extracted from meat, using acetone/ethanol (1:1 v/v), and determined fluorophotometrically. Data are expressed as means \pm SDs of triplicate experiments. Intact pieces of porcine muscle after incubation were exposed to white light (B) or UV light in a dark room (C), and then, the images were observed. The pink color indicates the production of Zn-protoporphyrin.

the mixture did not change in the formation of Zn-protoporphyrin, indicating that zinc ions are present at sufficiently high levels in meat²⁰ for the zinc ion-insertion reaction to proceed (Figure 4B). When meat as a substrate material was used, a considerable amount of Zn-protoporphyrin was formed without ascorbic acid, and the addition of ascorbic acid (6 mM) showed enhancement on the formation (Figure 4C). Figure 5 shows the change in the composition of heme and Zn-protoporphyrin in meat by the incubation with yeast FECH. At the initial time, heme was the main component of porcine muscle, but the amount of Zn-protoporphyrin increased sharply to 73% of the initial content of heme, whereas heme was decreased to 27%. These results indicated that the addition of the recombinant yeast FECH with ascorbic acid effectively enhanced the conversion reaction from heme in meat to Zn-protoporphyrin.

Formation of Zn-protoporphyrin from Heme in the Intact Piece of Porcine Muscle. The above results demonstrated that FECH is effective for the formation of Zn-protoporphyrin using a small amount of meat with the liquid reaction mixture. We finally examined the conversion using the intact piece of meat (15 g) as a reaction source. The solution (1 mL) containing yeast FECH (1 μ g) and 6 mM ascorbic acid was injected into muscle, and the treated meat was then incubated anaerobically. As shown in Figure 6A, the formation of Zn-protoporphyrin in the muscle was observed after 24 h of incubation at 30 °C. Zn-protoporphyrin was formed in samples either with or without ascorbic acid. In addition, a considerable amount of protoporphyrin in meat was also formed. The photomages indicated a bright red color of meat that emerged upon direct exposure of meat to both visible and UV light (Figure 6B,C). This proves that yeast FECH acts as a promoter of the conversion reaction to Zn-protoporphyrin from heme in meat.

DISCUSSION

The present study first demonstrated that highly efficient iron removal and subsequent conversion of heme in meat to Zn-protoporphyrin occur upon a relatively short period of incubation, via the catalysis of FECH. The replacement of iron by zinc in the formation of Zn-protoporphyrin was noted previously.^{15–17} Our previous studies^{11,12} showed that the formation of Zn-protoporphyrin can take place via the reverse and conversion reactions and was catalyzed by FECH. However, the level of production of Zn-protoporphyrin from heme is low because the reaction of FECH precisely proceeds to the metal ion-insertion (forward) reaction. We also found that a considerable concentration of reducing reagents including ascorbic acid and cysteine under anaerobic conditions was required for the highly efficient production of Zn-protoporphyrin. In addition, the use of recombinant FECH enhanced the conversion reaction of heme, with hemin, hemoglobin-heme, and myoglobin-heme as well as heme in meat strongly suggesting that FECH can catalyze the conversion reaction from any heme in tissues.

The formation of Zn-protoporphyrin without the decrease of heme was previously noted using exogenous myoglobin or meat extracts,²¹ indicating that the formation could follow the other pathway independent of FECH catalysis. On the other hand, we previously¹¹ reported that 67% of pigment of dry-cured ham was Zn-protoporphyrin, only 10% was heme, and the rest was protoporphyrin. The present study demonstrated that about 70% of metalloporphyrin in meat was Zn-protoporphyrin, which was accompanied by the decrease of heme after 24 h of incubation with yeast FECH at 30 °C (Figure 5). These results confirmed that endogenous porcine FECH in meat is responsible for the formation of Zn-protoporphyrin, and the formation of Zn-protoporphyrin is dependent upon the initial heme concentration in dry-cured ham including Parma ham.

We previously reported that the iron-removal activity of heme with mouse FECH upon a short period of incubation had an optimum temperature of 45 °C.^{12,19} Thus, we tried to use FECH of thermophilic bacteria for the formation of Zn-protoporphyrin because enzymes in these bacteria are relatively stable at high temperature. We expressed the recombinant FECH of *T. thermophilus* in *E. coli* and purified it. When the conversion of heme to Zn-protoporphyrin with *T. thermophilus* FECH was examined at 45 °C, the activity was unexpectedly low (data not shown). The bacterial enzyme activity was about 10% of that of the porcine

enzyme (Figure 1B). *E. coli* FECH was also examined for the conversion activity but was ineffective on the activity (data not shown). Among the enzymes examined, yeast FECH showed the highest activity.

It is known that mammalian FECH includes an iron–sulfur cluster at the carboxyl terminal. At present, the roles of the cluster are not fully understood. This cluster could play an important role in mammalian FECH activity.^{26,27} The cluster can also be found in FECH from some kinds of bacteria and yeast *Schizosaccharomyces pombe*,²⁸ but its role is not clear. We compared the stability of the cluster-free FECH of the bacterium *T. thermophilus*, the yeast *S. cerevisiae*, and the porcine enzyme containing the cluster. Although the iron–sulfur cluster could not be related to the ability of the reverse and conversion reactions of FECH, the differences in stability of bacterial, mammalian, and yeast FECH could be related to the presence of the cluster. Oxygen, nitric oxide, and various chemicals can easily destroy the iron–sulfur cluster.²⁶ This was supported by the observations that the formation of Zn-protoporphyrin was decreased by the addition of nitrite in the processing of dry-cured ham.^{17,21} Therefore, the mammalian FECH was unstable as compared with those of yeast and bacteria. The yeast FECH was quite stable with high activity (Figure 1B). Thus, yeast FECH can be the model supplement enzyme to obtain a high yield in the conversion of Zn-protoporphyrin from heme.

Ascorbic acid has been used as a preserving additive in meat products.²⁹ As shown previously, reducing systems can play a vital role in the reverse and conversion reactions of FECH. NADH-cytochrome *b*₅ reductase (metmyoglobin reductase) can reduce heme to enhance the reverse reaction.¹¹ In vitro, ascorbic acid and cysteine showed the same effect as NADH-cytochrome *b*₅ reductase on the reduction of ferric ions to ferrous ions, and then, the FECH can attack to remove ferrous ions in heme. In addition, ascorbic acid as well as cysteine at 6 mM can highly promote the reverse and conversion activities of FECH (Figure 3A). The enhancing ability of ascorbic acid on the formation of Zn-protoporphyrin found in this study is in agreement with another finding¹⁸ that ascorbic acid can promote the formation of the pigments of dry-cured ham. The decrease of FECH activity at a higher concentration of ascorbic acid can be explained by the decrease of pH value. On the other hand, the formation of Zn-protoporphyrin in meat via the conversion reaction occurred without any addition of exogenous reductants, showing that some reducing systems in meat are present at a significant level or can be derived from some kinds of bacteria. The endogenous reductants such as ascorbic acid, glutathione, and nicotine nucleotides in meat can help the endogenous FECH-dependent occurrence of iron-removal and the zinc ion-insertion reactions of heme in meat during the processing of ham.

Other investigators^{17,18} reported that the treatment of meat with NaCl improved the formation of Zn-protoporphyrin in dry-cured ham. A similar ability of salts was also found in the reaction system using meat extracts as FECH sources.¹⁸ In these studies, because zinc ions and protoporphyrin were added to the reaction mixture, the formation of Zn-protoporphyrin could only occur via the forward reaction. In contrast, the present study showed that NaCl did not have any effects on the formation of Zn-protoporphyrin via the reverse and conversion reactions from hemoproteins catalyzed by FECH. The reason for this difference is unclear, but it is possible that the enhancement of the zinc-insertion reaction by NaCl contributed to different enzyme sources and experimental conditions. The other possibility is that

the NaCl in ham maintains suitable growing conditions for yeast and some kinds of bacteria, which can enhance the formation of Zn-protoporphyrin in dry-cured ham.⁸ However, the formation of Zn-protoporphyrin slightly decreased in the antibiotic-treated samples,¹⁴ indicating that bacteria showed minor roles in the conversion reaction of Zn-protoporphyrin in dry-cured ham processing. Otherwise, it is possible that the addition of NaCl to meat during ham processing can prevent the growth of spoiling bacteria.³

Zinc ions can compete with iron in the insertion of divalent metal ions to protoporphyrin to form the corresponding metalloprotoporphyrin.³⁰ In the case of reverse and conversion reactions of heme, the amount of protoporphyrin is lower than that of Zn-protoporphyrin in the same reaction condition, indicating that zinc ions can enhance the removal reaction to remove the protoporphyrin, a substrate of the forward reaction. When porcine meat was used, the high level of conversion of heme to Zn-protoporphyrin occurred without the addition of exogenous zinc ions, indicating that zinc ions are abundant in meat²⁰ and are present at sufficient levels for the conversion reaction of heme to Zn-protoporphyrin. The amount of Zn-protoporphyrin formed in meat by incubation at 4 °C was less than that by incubation at 30 °C. This result agreed with the findings that the level of Zn-protoporphyrin did not increase considerably at low temperature during the incubation and production of dry-cured ham, and it just increased during the midtemperature incubation stage of the processing.¹³

It was reported that meat extracts acted as the enzyme sources for Zn-protoporphyrin formation,^{13,16,18} and the iron-removal and conversion reactions of myoglobin to Zn-protoporphyrin were successfully demonstrated.^{15–17} Although exogenous protoporphyrin, myoglobin, and zinc ions were added as substrates for these reaction mixtures, the yield in the formation was low. The present data showed that not only porcine FECH in porcine muscle (raw meat) but also yeast FECH as exogenously added enzyme used the endogenous myoglobin-heme in meat as a substrate, promoting the iron-removal and conversion reactions of heme to Zn-protoporphyrin.

The oxidation of protoporphyrinogen to protoporphyrin catalyzed by protoporphyrinogen oxidase occurs in vivo in the heme-biosynthetic pathway,³¹ and this protoporphyrin can be utilized for the formation of Zn-protoporphyrin. However, the sustained activity of the enzyme in meat in vitro has not been demonstrated yet, or the enzyme is unstable.³² Because the enzyme can be destroyed easily after cell death, this oxidation process probably did not occur during the processing of dry-cured ham, indicating that the insertion of zinc into protoporphyrin after the oxidation of protoporphyrinogen cannot regularly occur. Therefore, the replacement of iron by zinc ions occurs via the reverse, and conversion reactions of heme in meat cause the formation of Zn-protoporphyrin.

The present data on the conversion reaction from heme to Zn-protoporphyrin revealed that yeast recombinant FECH can shorten the period of formation of ham pigments with a high yield. The sensory quality of dry-cured ham consists of color, flavor, and texture. Flavor involves nonvolatile (taste) and volatile compounds (aroma) including free amino acids, peptides, fatty acids, and other natural organic compounds; texture relates to myofibrillar protein breakdown, extent of drying, degradation of connective tissues, and the intramuscular fat.³ The positive changes of flavor and texture properties can be developed up to 1–2 years of maturation and relate to the

proteolysis and lipolysis³ in which FECH could not be involved.

The conversion of hemoprotein-heme to Zn-protoporphyrin by FECH showed an optimum at pH 6.5 (Figure 2B), whereas pH in raw meats is 5.5–6.0.^{6,7} On the basis of the observations that the formation of Zn-protoporphyrin from myoglobin-heme readily proceeds in the raw tissues (Figures 5 and 6), some additional factors may be involved in the enhancement of the formation in meat. Yeast FECH showed the high conversion and iron removal activities at high NaCl concentration (up to 500 μ M) (Figure 3B). This demonstrates that the enzyme can be applied to dry-cured ham production, by the addition of 20–30 g NaCl/kg raw meat,³ in some stages to generate only the pigments, Zn-protoporphyrin, or protoporphyrin, of the ham.

Further studies will be carried out on the application of FECH to the dry-cured ham processing or that of other meat products to find suitable conditions for the enzyme reaction. Other studies should examine the effect of halophilic bacteria that can produce superior FECH or redox enzymes that are effective for the generation of ham pigments.

■ ASSOCIATED CONTENT

S Supporting Information. Figures of fluorescent profiles of Zn-protoporphyrin and protoporphyrin, effect of substrate concentrations on the conversion activity, and effect of reductants on the conversion activity. This material is available free of charge via the Internet at <http://pubs.acs.org>.

■ AUTHOR INFORMATION

Corresponding Author

*Tel/Fax: +81-75-724-7789. E-mail: taketani@kit.ac.jp.

Funding Sources

This study was supported in part by a grant from the Ministry of Education, Culture, Sport, Science and Technology of Japan and by grants from the Ministry of Health, Labor and Welfare of Japan.

■ ACKNOWLEDGMENT

We thank Drs. T. Numata and Y. Uebayashi for generously donating pig tissues.

■ REFERENCES

- Møller, J. K. S.; Skibsted, L. H. Nitric Oxide and Myoglobins. *Chem. Rev.* **2002**, *102*, 1167–1178.
- Pegg, R. B.; Shahidi, F. *Nitrite Curing of Meat: The N-Nitrosamine Problem and Nitrite Alternatives*; Food & Nutrition Press: Trumbull, CT, 2000.
- Toldrá, F.; Aristoy, M. C. Dry-Cured Ham. In *Handbook of Meat Processing*; Wiley-Blackwell: Hoboken, NJ, 2010; pp 351–362.
- Wakamatsu, J.; Nishimura, T.; Hattori, A. A Zn-porphyrin complex contributes to bright red color in Parma ham. *Meat Sci.* **2004**, *67*, 95–100.
- Taketani, S. Acquisition, mobilization and utilization of cellular iron and heme: endless findings and growing evidence of tight regulation. *Tohoku J. Exp. Med.* **2005**, *205*, 297–318.
- Adamsen, C. E.; Møller, J. K. S.; Hismani, R.; Skibsted, L. H. Thermal and photochemical degradation of myoglobin pigments in relation to colour stability of sliced dry-cured Parma ham and sliced dry-cured ham produced with nitrite salt. *Eur. Food Res. Technol.* **2004**, *218*, 403–409.
- Adamsen, C.; Hansen, M.; Møller, J.; Skibsted, L. Studies on the antioxidative activity of red pigments in Italian-type dry-cured ham. *Eur. Food Res. Technol.* **2003**, *217*, 201–206.
- Morita, H.; Niu, J.; Sakata, R.; Nagata, Y. Red pigment of parma ham and bacterial influence on its formation. *J. Food Sci.* **1996**, *61*, 1021–1023.
- Taketani, S. Molecular and genetic characterization of ferrochelatase. *Tohoku J. Exp. Med.* **1993**, *171*, 1–20.
- Ferreira, G. C. Ferrochelatase. *Int. J. Biochem. Cell Biol.* **1999**, *31* (10), 995–1000.
- Taketani, S.; Ishigaki, M.; Mizutani, A.; Uebayashi, M.; Numata, M.; Ohgari, Y.; Kitajima, S. Heme synthase (ferrochelatase) catalyzes the removal of iron from heme and demetalation of metalloporphyrins. *Biochemistry* **2007**, *46*, 15054–61.
- Chau, T. T.; Ishigaki, M.; Kataoka, T.; Taketani, S. Porcine Ferrochelatase: The Relationship between Iron-Removal Reaction and the Conversion of Heme to Zn-Protoporphyrin. *Biosci., Biotechnol., Biochem.* **2010**, *74*, 1415–1420.
- Parolari, G.; Benedini, R.; Toscani, T. Color formation in nitrite-free dried hams as related to Zn-protoporphyrin IX and Zn-chelatase activity. *J. Food Sci.* **2009**, *74*, C413–C418.
- Wakamatsu, J.; Okui, J.; Ikeda, Y.; Nishimura, T.; Hattori, A. Establishment of a model experiment system to elucidate the mechanism by which Zn-protoporphyrin IX is formed in nitrite-free dry-cured ham. *Meat Sci.* **2004**, *68*, 313–317.
- Ishikawa, H.; Kawabuchi, T.; Kawakami, Y.; Sato, M.; Numata, M.; Matsumoto, K. Formation of zinc protoporphyrin IX and protoporphyrin IX from oxymyoglobin in porcine heart mitochondria. *Food Sci. Technol. Res.* **2007**, *13*, 85–88.
- Ishikawa, H.; Yoshihara, M.; Baba, A.; Kawabuchi, T.; Sato, M.; Numata, M.; Matsumoto, K. Formation of zinc protoporphyrin IX from myoglobin with pork loin extract. *J. Fac. Agric., Kyushu Univ.* **2006**, *51*, 93–97.
- Adamsen, C. E.; Møller, J. K. S.; Laursen, K.; Olsen, K.; Skibsted, L. H. Zn-porphyrin formation in cured meat products: Effect of added salt and nitrite. *Meat Sci.* **2006**, *72*, 672–679.
- Parolari, G.; Benedini, R.; Raja, V. Zinc-protoporphyrin IX promoting activity in pork muscle. *LWT—Food Sci. Technol.* **2008**, *41*, 1160–1166.
- Taketani, S.; Tokunaga, R. Rat liver ferrochelatase. Purification, properties, and stimulation by fatty acids. *J. Biol. Chem.* **1981**, *256*, 12748–53.
- Jorhem, L.; Sundstrom, B.; Astrand, C.; Haeggglund, G. The Levels of Zinc, Copper, Manganese, Selenium, Chromium, Nickel, Cobalt, and Aluminum in the Meat, Liver and Kidney of Swedish Pigs and Cattle. *Z. Lebensm.-Unters. Forsch.* **1989**, *188*, 39–44.
- Wakamatsu, J.-i.; Okui, J.; Hayashi, N.; Nishimura, T.; Hattori, A. Zn protoporphyrin IX is formed not from heme but from protoporphyrin IX. *Meat Sci.* **2007**, *77*, 580–586.
- Lowry, O. H.; Rosebrough, N. J.; Farr, A. L.; Randall, R. J. Protein measurement with the Folin phenol reagent. *J. Biol. Chem.* **1951**, *193*, 265–75.
- Bradford, M. M. A rapid and sensitive method for the quantitation of microgram quantities of protein utilizing the principle of protein-dye binding. *Anal. Biochem.* **1976**, *72*, 248–54.
- Kohno, H.; Okuda, M.; Furukawa, T.; Tokunaga, R.; Taketani, S. Site-directed mutagenesis of human ferrochelatase: Identification of histidine-263 as a binding site for metal ions. *Biochim. Biophys. Acta* **1994**, *1209*, 95–100.
- Taketani, S. Measurement of Ferrochelatase Activity. In *Current Protocol in Toxicology*; Maines, M. D., Costa, L. C., Reed, D. J., Sassa, S., Sipes, J. G., Ed.; John Wiley & Sons, Inc.: New York, 1999; pp 8.7.1–8.7.8.
- Furukawa, T.; Kohno, H.; Tokunaga, R.; Taketani, S. Nitric oxide-mediated inactivation of mammalian ferrochelatase *in vivo* and *in vitro*: Possible involvement of the iron-sulphur cluster of the enzyme. *Biochem. J.* **1995**, *310* (Part 2), 533–538.
- Taketani, S.; Adachi, Y.; Nakahashi, Y. Regulation of the expression of human ferrochelatase by intracellular iron levels. *Eur. J. Biochem.* **2000**, *267*, 4685–4692.
- Dailey, T. A.; Dailey, H. A. Identification of [2Fe-2S] clusters in microbial ferrochelatases. *J. Bacteriol.* **2002**, *184*, 2460–2464.

- (29) Roig, M. G.; Rivera, Z. S.; Kennedy, J. F. *L*-Ascorbic acid: An overview. *Int. J. Food Sci. Nutr.* **1993**, *44*, 59–72.
- (30) Hunter, G. A.; Sampson, M. P.; Ferreira, G. C. Metal ion substrate inhibition of ferrochelatase. *J. Biol. Chem.* **2008**, *283*, 23685–23691.
- (31) Nishimura, K.; Taketani, S.; Inokuchi, H. Cloning of a human cDNA for protoporphyrinogen oxidase by complementation in-vivo of a hemG mutant of *Escherichia coli*. *J. Biol. Chem.* **1995**, *270*, 8076–8080.
- (32) Taketani, S.; Yoshinaga, T.; Furukawa, T.; Kohno, H.; Tokunaga, R.; Nishimura, K.; Inokuchi, H. Induction of terminal enzymes for heme-biosynthesis during differentiation of mouse erythroleukemia-cells. *Eur. J. Biochem.* **1995**, *230*, 760–765.

False-Positive Accumulation of Metaiodobenzylguanidine in a Case with Acute Intermittent Porphyrria

Tomoko Masuda¹, Rie Ota¹, Takao Ando¹, Naoto Maeda², Yutaka Horie³,
Toshiro Yoshimura¹, Masakatsu Motomura¹ and Atsushi Kawakami¹

Abstract

We report a 36-year-old woman presenting with hypertensive encephalopathy followed by bulbar palsy and quadriplegia. After an extensive screening for secondary causes of hypertension, the patient was suspected of having pheochromocytoma due to increased levels of catecholamines in the plasma and the urine, and positive ¹³¹I-metaiodobenzylguanidine (MIBG) accumulation in the gallbladder. However, MIBG accumulation was not reproducible without any tumors accompanying this accumulation in the gallbladder. A diagnosis of acute intermittent porphyria was finally confirmed based on the characteristic pictures, increased urinary excretion of porphobilinogen, and identification of a heterozygous missense mutation of R173W in the hydroxymethylbilane synthase gene. This case highlights a pitfall in utilizing MIBG to detect a source of excessive catecholamine and also suggests the importance of having a complete clinical history and extensive work-up of any possible differential diagnosis. We also review the potential mechanism by which false-positive MIBG accumulation occurs.

Key words: acute intermittent porphyria, MIBG, pheochromocytoma, false-positive

(Intern Med 50: 1029-1032, 2011)

(DOI: 10.2169/internalmedicine.50.5096)

Introduction

Metaiodobenzylguanidine (MIBG) has been widely used as a clinical tool to detect and localize pheochromocytoma since MIBG selectively accumulates in cells derived of neuroectodermal origin, including pheochromocytoma (1). It has been shown that the specificity of MIBG accumulation, when used to localize clinical pheochromocytomas, is as high as 95-100% (2). Reflecting excessive secretion of catecholamines from tumors, clinical symptoms seen in patients with pheochromocytoma are headache, anxiety, weight loss, nausea, and paroxysmal hypertension.

Acute intermittent porphyria (AIP) is characterized by episodic acute attacks of abdominal pain, headache, paroxysmal hypertension, seizures, confusion and hallucinations. Acute porphyria attacks can be life-threatening, since the motor polyneuropathy occasionally progresses to respiratory

failure requiring a mechanical ventilator. Patients suffering from AIP, however, can be totally asymptomatic during the remission periods. This is because AIP is caused by reduced enzyme activity of hydroxymethylbilane synthase involving the heme biosynthesis, and excessive accumulation of neurotoxic heme precursors is only seen during and shortly after the attacks.

As described above, there is an overlap between such clinical symptoms of AIP and those of pheochromocytoma as paroxysmal hypertension and headache, and thus patients with AIP can be misdiagnosed with pheochromocytoma or vice versa. Here, we report a case of AIP with a confusing finding of false-positive MIBG accumulation suggesting pheochromocytoma. We also review the putative mechanisms involved in the false-positive MIBG accumulation.

¹The First Department of Medicine, Nagasaki University Graduate School of Biomedical Sciences, Japan, ²The Second Department of Internal Medicine, Tottori University Faculty of Medicine, Japan and ³Department of Gastroenterology, Shimaneken Saiseikai-Gotsu General Hospital, Japan

Received for publication January 1, 2011; Accepted for publication January 12, 2011

Correspondence to Dr. Takao Ando, takaoando@gmail.com

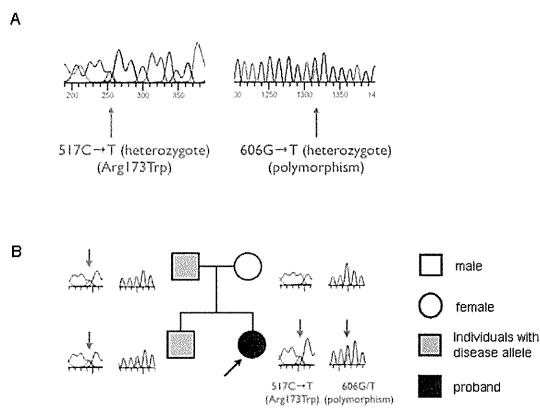


Figure 1. Identification of a missense mutation in hydroxymethylbilane synthase in the patient and her family members. (A) Genomic DNA taken from peripheral blood mononuclear cells were PCR-amplified with specific primers for the hydroxymethylbilane synthase gene and the PCR products were directly sequenced as described previously (20). A missense mutation of R173W is indicated by a red arrow and polymorphism of 606G to T is indicated by the blue arrow. (B) Genetic testing of the family members identified the disease allele in the father and sibling of the proband. The proband is indicated by the black arrow.

Case Report

A 36-year-old woman was admitted to the regional hospital in our area because of acute onset of visual field loss caused by hypertensive encephalopathy. While her visual field loss gradually improved by vigorous anti-hypertensive treatment, she developed progressive quadriplegia and bulbar paralysis and was therefore transferred to our university hospital. Her past medical history was unremarkable except for frequent episodes of headaches, nausea, vomiting, and generalized body pain associated with paroxysmal hypertension during the premenstrual period for more than ten years.

On physical examination, she was dehydrated and urinating port wine-colored urine. Additionally, there was apparent bulbar paralysis and quadriplegia associated with a loss of deep tendon reflexes. Since the patient was intubated and under sedation, we were not able to ask her whether she had sensation in her limbs. A blood test showed moderate anemia and the anti-ganglioside antibodies studied were negative. Cerebrospinal fluid analysis was normal. Nerve conduction study in the median, ulnar, peroneal, and tibial nerve showed normal conduction velocity with a low amplitude (amplitude and velocity was 0.79 mV and 44.0 m/sec in the median nerve and 1.5 mV and 46.4 m/sec in the ulnar) indicating axonal motor polyneuropathy while there was no involvement of sensory nerves. From the clinical picture of the patient, we strongly suspected an attack of acute porphyria. This was supported by a markedly elevated urinary concentration of porphobilinogen (134.2 mg/day; reference range less than 2 mg/day). Other urinary porphy-

rins were also increased; 5-aminolevulinic acid (22.3 mg/L; reference range <5 mg/L), uroporphyrin (1,820 μg/gCr; reference range <36 μg/gCr) and coproporphyrin (8,540 μg/gCr; reference range 170 μg/g Cr). After obtaining written informed consent from the patient and her family and approval from the ethical committee at Tottori University Hospital (Tottori, Japan), we were also able to detect a heterozygous mutation in the hydroxymethylbilane synthase gene (R173W caused by 517C to T in exon 10), which confirmed the diagnosis of AIP (Fig. 1A). There was an additional polymorphism of 606 G to T (Fig. 1A), and genetic testing of her family members revealed that the disease allele was paternally inherited (Fig. 1B). The patient was treated with intravenous hyperalimentation, cimetidine, and chlorpromazine, and the neurological signs and symptoms gradually improved.

Before being transferred to our hospital, the patient was extensively investigated for the possibility of secondary hypertension as an etiology of hypertensive encephalopathy. Plasma levels of catecholamines and urinary levels of catecholamine metabolites were found to be elevated: plasma adrenaline (242 pg/mL; reference range <100 pg/mL), noradrenaline (2,583 pg/mL; reference range 100 to 450 pg/mL), dopamine (231 pg/mL; reference range <20 pg/mL) and urinary metanephrine (0.22 mg/day; reference range 0.04 to 0.19 mg/day), normetanephrine (1.37 mg/day; reference range 0.09 to 0.33 mg/day), VMA (9.0 mg/day; reference range 1.5 to 4.3 mg/day). Therefore, a diagnosis of pheochromocytoma was considered and ¹³¹I-MIBG scintigraphy showed positive accumulation in the gallbladder (Fig. 2A, 2B). However, we were not able to find any tumorous lesions in or near the gallbladder by ultrasound (Fig. 2C). ¹²³I-MIBG accumulation studied 14 days after the ¹³¹I-MIBG study showed no accumulation of MIBG in the gallbladder or adrenal gland (Fig. 2D), and there was a gradual decrease of urinary metanephrine.

Discussion

The case reported here was first presented with hypertensive encephalopathy caused by paroxysmal hypertension subsequently complicated with bulbar palsy and quadriplegia as a result of axonal motor polyneuropathy. The diagnosis of AIP was made based on the characteristic clinical presentation, increased urinary excretion of porphobilinogen, and genetic testing. It has been shown that mutations were widely distributed within the gene coding hydroxymethylbilane synthase, and the mutation identified in the present patient was also observed in Caucasians as well as in other unrelated Japanese patients with AIP (3-5). It has also been shown that the mutation is the substitution of an essential arginine to tryptophan in the active site of the enzyme, decreasing catalytic activity (<1%) (6). The patient could have been incorrectly diagnosed with pheochromocytoma based on her paroxysmal hypertension and false-positive accumulation of ¹³¹I-MIBG. A misdiagnosis of this kind can easily occur in

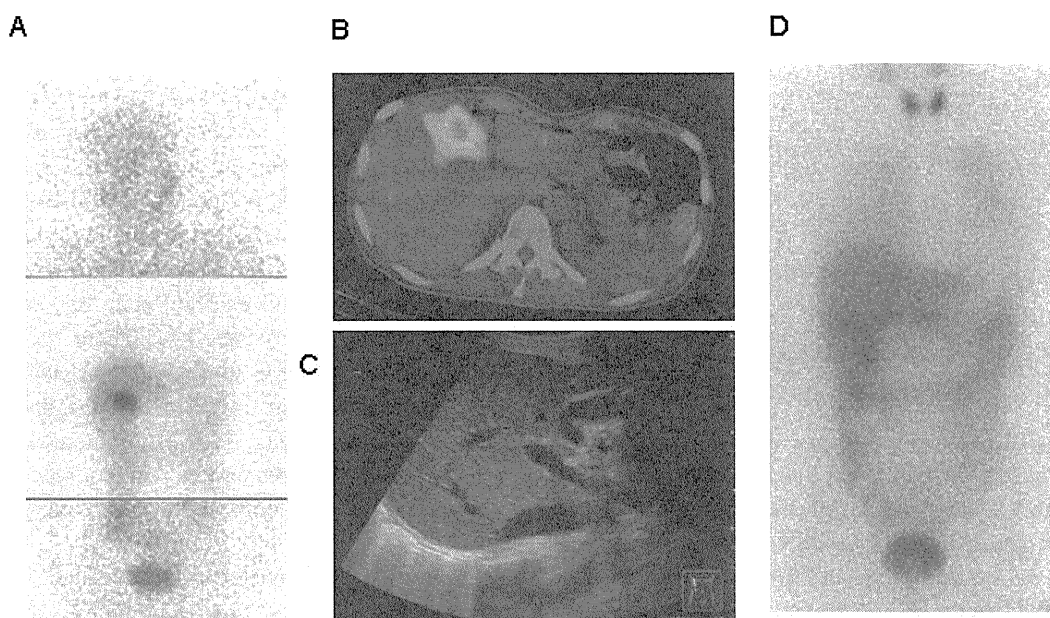


Figure 2. False-positive accumulation of MIBG in the gallbladder. There is clear accumulation of ^{131}I -MIBG in the right upper abdomen (A), which corresponds to the gallbladder, as shown in SPECT (B). There was no detectable tumor in or near the gallbladder on ultrasound (C). ^{123}I -MIBG scintigraphy taken 14 days after ^{131}I -MIBG showed no abnormal accumulation (D).

Japan, where AIP is extremely rare [up to 198 cases of AIP have been diagnosed as of 2009 (7)]. In addition, the clinical presentation of pheochromocytoma can vary greatly and mimic signs and symptoms seen in many other disorders (2).

It has been shown that acute porphyria attacks are commonly seen in females, although very rarely before puberty and after menopause, with a peak occurrence within the third decade (8, 9). Most patients have one or two attacks and then fully recover without a recurrence for the rest of their lives, but less than 10% develop recurrent acute attacks. During the acute attacks, reflecting augmented sympathetic activity, tachycardia, excessive sweating, and hypertension are commonly present (10). As shown herein, increased catecholamine production can be detected and may possibly suggest an incorrect diagnosis. When an acute attack of porphyria is suspected, it is essential to obtain a complete clinical history, perform an extensive work up of any possible differentiating diagnosis, and determine the urinary concentration of porphobilinogen (11).

MIBG is a norepinephrine analogue which is taken up by neuroendocrine cells through an active mechanism and stored in the neurosecretory granules. This leads to a specific concentration of the molecule in the neuroendocrine cells (1). Only limited reports of false-positive uptake in other lesions have been published. One major cause of false-positive findings is urinary tract retention, since the reagent is excreted in the urine (12). Other rare false-positive MIBG accumulations have been reported in the adrenal gland with adenoma (13), carcinoma (14) or metastatic choriocarcinoma, and adenomatous polyp of the cecum, infantile myofibromatosis (15), pancreaticoblastoma (15), acute focal

pyelonephritis, hepatic hemangioma, hepatocellular carcinoma (16), and juvenile capillary hemangioma (17). The non-specific accumulation of MIBG is thought to be mediated by a passive uptake and diffusion. It has been shown that non-specific uptake tends to disappear more rapidly than specific uptake (15). An augmented blood flow and enhanced diffusion of MIBG within the tumor could be putative mechanisms of false-positive MIBG uptake and accumulation in non-neuroendocrine tumors (15, 18).

There was false-positive accumulation of MIBG in the gallbladder in the case with AIP reported here. To our knowledge, there is no report of a similar false-positive MIBG accumulation. The accumulation of MIBG in the gallbladder can be considered a characteristic finding in patients with AIP. Since the liver is one of the major organs involving heme biosynthesis, which is partially defective in AIP, MIBG clearance might be disturbed during acute attacks of AIP. It is not known whether MIBG accumulates in any specific organ in patients with AIP. False-positive MIBG accumulation in the normal adrenal gland in a patient with AIP has in fact been reported (19). Thus, it seems unlikely that MIBG tends to accumulate in the gallbladder in AIP although there have been no studies confirming this. The other possibility is that the critical condition of the patient reported herein might have influenced the blood flow of the gallbladder, as the patient was severely ill and receiving intravenous hyperalimentation when ^{131}I -MIBG accumulation was studied. We were not able to find any studies on the blood flow of the gallbladder in patients with intravenous hyperalimentation, in which the gallbladder is known to dilate. However, the increased blood flow in the gallbladder would not have been the cause of false-positive MIBG accu-